NAVAL POSTGRADUATE SCHOOL

Monterey, California

THESIS

STABILITY AND CONTROL
FLIGHT TESTING OF A HALF-SCALE
PIONEER REMOTELY PILOTED VEHICLE

by

Kent Robert Aitcheson

September, 1991

Thesis Advisor: Prof. Richard M. Howard

Approved for public release; distribution is unlimited

REPORT DOCUMENTATION PAGE

1a Report Security Classification: Unclassified
1b Restrictive Markings
2a Security Classification Authority
3 Distribution Availability of Report: Approved for public release; distribution is unlimited.
2b Declassification/Downgrading Schedule
4 Performing Organization Report Number(s)
5 Monitoring Organization Report Number(s)
6a Name of Performing Organization: Naval Postgraduate School
6b Office Symbol (*If Applicable*): 67
7a Name of Monitoring Organization: Naval Postgraduate School
6c Address (*city, state, and ZIP code*): Monterey, CA 93943-5000
7b Address (*city, state, and ZIP code*): Monterey, CA 93943-5000
8a Name of Funding/Sponsoring Organization
8b Office Symbol (*If Applicable*)
9 Procurement Instrument Identification Number
8c Address (*city, state, and ZIP code*)
10 Source of Funding Numbers

Program Element Number	Project No	Task No	Work Unit Accession No

11 Title: Stability and Control Flight Testing of a Half-Scale Pioneer Remotely Piloted Vehicle
12 Personal Author(s): Aitcheson, Kent R.

13a Type of Report	13b Time Covered		14 Date of Report (*year, month,day*)	15 Page Count
Master's Thesis	From	To	1991 September 25	75

16 Supplementary Notation: The views expressed in this thesis are those of the author and do not reflect the official policy or position of the Department of Defense or the U.S. Government.

17 Cosati Codes			18 Subject Terms (*continue on reverse if necessary and identify by block number*)
Field	Group	Subgroup	RPV, Longitudinal Stability, Directional Stability, Telemetry

19 Abstract (*continue on reverse if necessary and identify by block number*)

Stability and control flight testing was conducted on a half-scale Pioneer remotely piloted vehicle. The aircraft was instrumented with sensors to measure flight control deflections, angle of attack, side slip angle, and airspeed. A developmental telemetry transmitter was installed to send the information to a ground based receiver where it was recorded for computer processing. Flight tests were conducted to characterize longitudinal static stability by varying the center of gravity to determine the neutral point. Directional static stability was characterized using steady heading side slip flight tests. The telemetry system's performance was acceptable and the directional stability data correlated favorably with data gathered from wind tunnel testing and computational methods. Longitudinal stability was more difficult to characterize due to limitations of elevator deflection resolution and the amount of data gathered. Additional flight testing will be conducted to tune the telemetry system with the data collection sensors, and to increase the Pioneer static stability data base.

20 Distribution/Availability of Abstract
[X] unclassified/unlimited [ ] same as report [ ] DTIC users
21 Abstract Security Classification: Unclassified

22a Name of Responsible Individual	22b Telephone (*Include Area code*)	22c Office Symbol
Richard M. Howard	(408) 646-2870	AA/Ho

DD FORM 1473, 84 MAR 83 APR edition may be used until exhausted
All other editions are obsolete

Approved for public release; distribution is unlimited.

STABILITY AND CONTROL FLIGHT TESTING OF A HALF-SCALE PIONEER REMOTELY PILOTED VEHICLE

by

Kent R. Aitcheson
Lieutenant, United States Navy
B.S., Whitworth College, 1983

Submitted in partial fulfillment of the requirements
for the degree of

MASTER OF SCIENCE IN AERONAUTICAL ENGINEERING

from the

NAVAL POS[illegible]

ABSTRACT

Stability and control flight testing was conducted on a half-scale Pioneer remotely piloted vehicle. The aircraft was instrumented with sensors to measure flight control deflections, angle of attack, side slip angle, and airspeed. A developmental telemetry transmitter was installed to send the information to a ground based receiver where it was recorded for computer processing. Flight tests were conducted to characterize longitudinal static stability by varying the center of gravity to determine the neutral point. Directional static stability was characterized using steady heading side slip flight tests. The telemetry system's performence was acceptable and the directional stability data correlated favorably with data gathered from wind tunnel testing and computational methods. Longitudinal stability was more difficult to characterize due to limitations of elevator deflection resolution and the amount of data gathered. Additional flight testing will be conducted to tune the telemetry system with the data collection sensors, and to increase the Pioneer static stability data base.

C.1

TABLE OF CONTENTS

LIST OF SYMBOLS

ρ	Density
μ	Fluid Viscosity
PMARC	Panel Method Ames Research Center
C_L	Lift Coefficient
C_M	Moment Coefficient
Vdc	Volts, Direct Current
mAh	Milli-Amp Hours
NiCd	Nickel-Cadmium
α	Angle of Attack
β	Side Slip Angle
δ_a	Aileron Deflection
δ_e	Elevator Deflection
δ_r	Rudder Deflection
KIAS	Knots Indicated Airspeed
mVdc	Milli-Volts, Direct Current
ms	Milli-Seconds
C_{M_α}	Moment Coefficient Curve Slope
$C_{M_{owb}}$	Moment Coefficient of the Wing-Body
h	Center of Gravity as a Percentage of MAC
MAC	Mean Aerodynamic Chord Length

ACKNOWLEDGMENTS

I would like to extend my sincerest appreciation to all of those people who helped bring this project to a successful conclusion. Special thanks are extended to Mr. Tom Christian for his electronics expertise and for his persistence with the CHOW-1G. Mr. Don Meeks has been an immeasurable resource in solving the myriad of problems associated with modifying the Pioneer. He is also one heck of an R/C pilot with more "Dead Stick" time than most others have as total flight time. LCDR Kevin Wilhelm deserves special thanks for service above and beyond that expected from an equally busy colleague. Lastly, I can't thank Dr. Richard Howard enough for his extreme patience with myself and for his nurturing of flight test at the Naval Postgraduate School.

My greatest thanks go to my wife, Juli, for her love, understanding, and perseverance; also, to my son, Robert, and my daughter, Erin. I don't know how they do it.

I. INTRODUCTION

In his book "On War", Clausawitz discusses intelligence in war. He postulated that once war began information would become slowed, tangled, and in general, untrustworthy. He said that "many intelligence reports are contradictory; even more are false, and most are uncertain...the task becomes infinitely harder in the thick of fighting" [Ref. 1:pp. 117-118]. The efficient and accurate flow of information has always presented problems to battle commanders and Clausawitz's theory has been proven many times. In particular, field and fleet commanders have especially needed accurate information on the position and strength of opposing forces, targeting and battle damage assessment.

When the military began to use aircraft, the capability of gathering information was greatly enhanced. Aircraft, including blimps that carried observers aloft, extended the ranges and heights necessary to increase the speed and accuracy of intelligence.

Along with increases in aircraft technology came increases in electronics technology. With the advent of radar in World War II, enemy aircraft and ships could be detected and located beyond visual range without endangering aircrew. Still, there were many limitations to these older systems. Ships could hide over the horizon and aircraft could hide behind terrain making them invisible to defenders. Ground forces were impossible to locate with radar and even heavy weather could degrade these systems' capabilities.

Inevitably, adversaries began to develop counter measures against these electronic and airborne assets. As aircraft became faster and more sophisticated, counter measures also improved at practically the same rate. By the end of the

Vietnam War, supersonic aircraft were flying over target areas after strikes to photograph battle damage. While doing so, they had to dodge high-speed surface-to-air missiles capable of several times the speeds and g-loadings, and at any altitude the reconnaissance aircraft could fly. However, before aircraft had the opportunity to fly over a target, even if the target were undefended, they had to be launched from ground bases or aircraft carriers. With bad weather or rough seas aircraft could not even get airborne.

Today, the capability of anti-aircraft missiles has increased even more to where they seem nearly impossible to defeat. As reconnaissance platforms became more complex their cost increased extraordinarily. With the increase in defense system capabilities and the possibility of losing aircrews and multimillion-dollar platforms, alternative methods of information gathering had to be made available.

In the 1970's and 80's, the use of satellites was coming into full swing and imaging from space was improving by leaps and bounds with fantastic results. The cost of satellite programs was just as impressive! As seen in the war with Iraq, any kind of cloud cover or other obscuration could degrade or eliminate expensive space-based assets. Field commanders could not afford to wait several days for storm fronts to pass to receive information, even if the news they finally received was crystal clear and 100% accurate. In the end, timeliness of information is usually as critical or more critical than accuracy. A need had developed for some type of intermediate, flexible, autonomous, low-cost intelligence gathering system. One solution to this problem was to initiate an unmanned air vehicle (UAV) program. Currently, the U.S. Navy is part of the joint armed services UAV program which is discussed in Chapter II.

II. BACKGROUND

A. HISTORY

The Pioneer Remotely Piloted Vehicle (RPV) was originally developed in Israel and is currently produced in the U.S. by AAI Corporation. In 1982, Unmanned Air Vehicles (UAV's) were used by the Israeli armed forces to locate and characterize Syrian surface-to-air missile sites using imagery and electronic warfare packages [Ref 2:p. 47]. This type of employment was truly a first in the history of war fighting and the results of these operations caused the U.S. military to take a serious interest in UAV's. In 1983, Commandant of the U.S. Marine Corps General P. X. Kelly, along with Secretary of the Navy John Lehman, realized the value of this type of system and initiated development of a UAV program. The 1st RPV Platoon was formed in 1985 and deployed aboard the amphibious helicopter carrier U.S.S. Guam [Ref. 3: p. 9].

The Pioneer reached a height of notoriety during operation Desert Storm. Marine Corps Commandant General Alfred Grey told Congress that "[the Pioneer] was extraordinarily successful." Six Pioneer tactical units were deployed: three were with Marine ground units, one was with the 7th Corps Army and one each deployed on the battleships Wisconsin and Missouri. Each unit operated five vehicles. Pioneer logged 1,011 hours during 307 flights and were equipped with either television or forward looking infrared (FLIR) cameras for day and night operations [Ref. 4: p.86].

Pioneer was used for everything from spotting naval gun fire from the battleships during shore bombardment to flying strike aircraft and helicopter low

level routes prior to actual missions. This latter mission gave aircrew the opportunity to preview the route's terrain and identify the target and any threats that might have been present. During the conflict, two Pioneers were lost to anti-aircraft artillery (AAA) while three were hit and damaged but were retrieved, repaired and returned to service. Five were lost to non-combat related causes [Ref. 4: p.86].

Pioneer is a very capable system. The full-scale version has a 17-foot wingspan and weighs 420 pounds. Maximum speed is about 115 miles per hour and the vehicle can operate up to an altitude of 15,000 feet. It has a range of about 100 nautical miles and over four hours of endurance. However, in 1988, huge cost overruns by Lockheed on the Aquila system prompted Congress to put a freeze on all RPV procurements [Ref. 3:pp. 10-11]. These problems put a halt to UAV procurement but with the overwhelming success of Pioneer in the war with Iraq, the future of UAV's would seem to be secure.

B. DYNAMIC MODELING

Scale models go well beyond being entertainment for hobbyists and can be considered precise engineering tools when properly constructed. Ideally, the engineer should strive to create a dynamically similar model which is "one whose size, propulsive power, weight and weight distribution are all in scale with the full size aircraft being simulated [and] responds to inertial as well as aerodynamic forces." The scaling factor (λ) is defined as the reciprocal of the linear scale. Thus, for a half- scale model the scaling factor is $\lambda=2$. If a model is made as large as possible (small λ) weight scaling is easier, Reynolds number is easier to control, reactions to control inputs are more realistic and moments of inertia will be more accurate [Ref. 5:pp. 30-31]. The half-scale Pioneer model

used at the Naval Postgraduate School (NPS) is geometrically similar to the full-scale version except it does not have the new extended horizontal stabilizer as on the full-scale unit. The half-scale is not designed to be dynamically scaled for weight or moments of inertia, however. Since static stability and control parameters were the characteristics under consideration for this study, dissimilar dynamics was not a concern.

For air flows to be similar, two of the more critical parameters that must be controlled are Reynolds number (Re) and Mach number (M) [Ref. 6:p. 27]. The Reynolds number is a dimensionless parameter that incorporates density, velocity, size and viscosity, all of which contribute to the energy state of a flow. The equation for the Reynolds number is $Re=\rho Vc/\mu$ (or Vc/ν where ν is the kinematic viscosity μ/ρ). Friction forces dominate when Re is low. Low Reynolds number is a characteristic of slow speed, small reference length (reference length for an aircraft is usually the wing chord length) and lower densities (such as those experienced in high altitude flight). Inertial forces dominate when Re is high. High Reynolds numbers are associated with fast speed and higher densities (such as in low altitude flight). Reynolds number is commonly used to compare different flows and to characterize whether the flows are laminar, turbulent or somewhere in transition. Mach number is the ratio of free stream velocity to sonic velocity.

The influence of the two factors just described cause scale models to suffer increased drag and decreased lift at their relatively low flight velocities. To minimize these effects, Hall suggested that Re for a model be kept greater than 120,000 (the higher, the better) to avoid the penalties of friction drag and laminar flow separation [Ref. 5:p. 32]. Since the half-scale Pioneer flies at

airspeeds that constitute negligible Mach number, Re is the most important parameter to control. At an airspeed of 60 miles per hour on a standard day at sea level (typical flight condition for the half-scale Pioneer) the Reynolds number is approximately 545,000 based on the chord length of the wing. This is sufficiently above the suggested 120,000 limit to avoid the penalties associated with low energy airflow.

C. NAVAL POSTGRADUATE SCHOOL INVOLVEMENT

To update and improve the Pioneer RPV and other UAV systems, the Pacific Missile Test Center (PMTC) at Pt. Mugu, California has been designated in the Unmanned Aerial Vehicles Joint Project charter to be the test and evaluation center for all joint projects. The Naval Postgraduate School (NPS) in Monterey, California acts in support of the UAV office at PMTC through tests and evaluation with scaled models, wind-tunnel testing and numerical modeling.

A wind-tunnel test related to the half-scale Pioneer was conducted at NPS by Tanner in March, 1989, to determine propeller efficiencies and thrust coefficients for drag studies [Ref. 9:pp. 51-56]. Bray assisted the Target Simulation Lab at PMTC in conducting wind-tunnel tests on a 0.4-scale model at Wichita State University to determine the static stability and control derivatives for use in simulation for UAV training [Ref. 8:p. 33].

Flight testing has been on going at NPS for several years, as well. Tanner also conducted flight tests of the half-scale model from which the drag polar was constructed [Ref. 5:pp. 27-29]. Salmons initiated static longitudinal and directional stability flight testing in September, 1990. Current flight testing continues the longitudinal and directional stability tests conducted by Salmons using an updated and refined data collection system described in detail later.

Future flight testing will be designed to investigate the dynamic qualities of the Pioneer. Plans are also being considered to replace the current Clark Y airfoil with a new design in hopes of increasing performance and to add a new tail to better simulate the full-scale Pioneer's configuration.

Computational modeling was initially conducted by Lyons in June, 1989. Using the low-order panel method code PMARC obtained from NASA-Ames Research Center, he determined the curves for lift coefficient (C_L) and moment coefficient (C_M) versus angle of attack (α) along with other measures of longitudinal and directional stability and control. He was also able to predict the drag polar using drag build-up techniques and induced-drag results from his numerical work [Ref. 9:pp. 11-48]. Plans for future computational experiments include using a parameter-estimation scheme along with flight test data to improve the predicted values of the stability and control derivatives of the Pioneer. With accurate estimates for these derivatives, a valid model for the motion of the full-scale Pioneer can be developed. An accurate model would allow programming a simulator for improved aircraft operator training, reducing the risk of losing an aircraft.

D. SCOPE

As mentioned, static stability flight testing of the half-scale Pioneer was initiated by Salmons in September, 1990. The aim of his investigation was to determine the neutral point and to characterize directional stability [Ref. 10:pp. 23-25]. Several problems were identified pertaining to his tests. Primarily, vibration caused high-frequency g-loading which interfered with the seven channel data recorder carried in the aircraft fuselage. A suspension system was engineered to reduce the affect of vibration but data collection was still impaired.

Vibration was great enough to cause significant scatter of the data which precluded drawing definite conclusions about the characteristics of the aircraft.

Another problem with the previous configuration of the half-scale model was the use of the flight control servos as data collection instruments. Small potentiometers inside the servos were wired to measure voltage changes as the control surfaces were displaced. With these two systems combined, the possibility of loss of controlled flight caused by interference between them caused some concern. Also, the voltage range of the servo potentiometers was quite narrow (less than one volt). That is, each degree of control surface deflection produced a very small change in voltage output. Lastly, the reference voltage to each servo was different, resulting in a lack of standardized output.

Some of the problems encountered by the full-scale Pioneer have included apparent autopilot-related pitch instability at high altitudes as well as limited lateral control and degraded maneuverability during the approach flight phase [Ref 11: p. 4.4-1]. Currently NPS operates its half-scale model of the Pioneer RPV to investigate these problems and act as a test bed for future projects.

The research for this report focused on investigating a means of effectively gathering data from which longitudinal and directional stability could be characterized. To accomplish these goals, modifications had to be made to the flight control and data collection systems to completely separate them into two independent systems. Then, to further increase the quality of data collection, a telemetry system, developed in separate research, was incorporated to eliminate the need to carry the cassette data recorder on board the aircraft. Once the hardware changes were made, flight testing was conducted to clarify the work begun by Salmons.

III. SYSTEMS

A. ELECTRICAL SYSTEM

The electrical system's original configuration used a single power source. A 4.8 Vdc, 4000 mAh, NiCd battery supplied power to the flight control radio receiver which distributed power to the flight control servos for control surface deflection. Power was simultaneously supplied to small potentiometers located inside the control servos. The servo cases had been opened and wires connected to these potentiometers so that measurements of voltage changes commensurate with control surface deflections could be made (this was not a function intended by the manufacturer). The system also had a dc to dc converter connected in parallel with the battery to convert its 4.8 volts to ±15 volts for powering the airspeed transducer. A circuit parallel to the dc to dc converter stepped down the 15 Vdc to 10 Vdc to power the α-β probe potentiometers [Ref. 10:p. 12].

Although the original arrangement seemed to be an efficient use of space and equipment, several problems arose. These problems included too great of a demand for power from the battery, too small of an output voltage gradient from the potentiometers inside the flight control servos, and concern about interference between the control function of the servo and the data collection function of the servo which might lead to loss of control of the aircraft. Also, there was no standardization of input voltage to the various data collection potentiometers.

The first step in correcting these problems was to separate the control system from the data collection system. Low-torque potentiometers were installed next

to one aileron, one rudder and the elevator and the leads to the flight control servo internal potentiometers were disconnected. While the previous arrangement required two output wires from each servo's internal potentiometer, the new configuration required three leads per potentiometer. One wire supplied power to the new units, one was for the variable "wiper" arm and another for the ground. A 5 Vdc power supply was provided by the newly incorporated telemetry transmitter unit to the new potentiometers (discussed further in Section C of this chapter). Previously, the control servo internal potentiometers received power from the battery through the radio control receiver when the control system was activated.

The above modifications resolved most of the problems previously outlined. The control system was completely separated from the data collection system, removing the possibility of losing control of the aircraft through interference. The 4.8 Vdc battery was used to power only the control receiver and to supply the dc to dc converter with power for the airspeed transducer. The 10 Vdc from the converter was no longer necessary for the α-β probe potentiometers since they were connected to the telemetry transmitter power source. The telemetry transmitter had its own 9.6 Vdc power supply which it converted to 5 Vdc to operate all of the data collection potentiometers. This modification reduced the demand on the 4.8 Vdc battery (considered to be the main battery) and standardized the input voltage to the potentiometers. The output voltage gradient from the potentiometers was enhanced using a gear system that is explained further in Section C.

In the original electrical system, each of the control servos (five, not including the flap servos) were wired to measure voltage changes from their

internal potentiometers. There were ten input wires from the five control surfaces and six more leads from the α-β probe and the airspeed transducer (two wires each) for a total of 16 leads for eight inputs. Also, at one time, there were sensors to measure engine rpm and the g-levels caused by vibration. A total of ten measurements were available for input to the data tape recorder at any given time. The data recorder could handle a maximum of seven inputs. To allow selection of the desired inputs for a particular flight test, a 16 switch selector board was designed and mounted in the aft end of the fuselage [Ref. 10:p. 46]. The new electrical system was fitted with a nine-wire ribbon for data collection from the three new control surface potentiometers and for direct input to the telemetry transmitter. The α-β probe and airspeed transducer inputs were retained and they also went directly to the transmitter. The remainder of the inputs were removed so that only six channels were necessary for data collection. To simplify the electrical system and reduce weight, the switching panel was removed.

Since the control servos and the data collection potentiometers were located at the control surfaces and the radio control receiver and telemetry transmitter were located in the fuselage, a disconnect system was needed to allow removal of the wing and the tail boom assembly from the body. Previously, clip-on type computer connectors were used that attached to the ribbon wire by pressing sharp, metal contacts through the insulators of each wire. The strong vibration levels of the aircraft caused several wires to fail and break contact. After replacing the old ten-wire ribbon with the new nine-wire ribbon, the old connectors for the data collection system and also for the 21-wire servo control system ribbon were removed. The old connectors were replaced with cannon

plugs that had soldered leads, each of which was wrapped in heat shrink, with the entire bundle supported inside the collar with foam rubber to reduce vibration strain. Overall, the modifications (which includes the installation of the telemetry transmitter) reduced the dry weight of the aircraft by one pound to a total of 31.3 pounds. Appendix A, Figure A.1, has the general wiring schematic for the new electrical systems.

B. FLIGHT CONTROL SYSTEM

The half-scale Pioneer is configured with ailerons, twin rudders, elevator and flaps, all of which are actuated by radio-controlled servos. The flaps were added to the half-scale model as a safety feature for landings and were not on the full-scale, operational vehicle. Two elevator configurations have been used on the full-scale Pioneer. The current operational aircraft has a horizontal stabilizer and elevator that extends outboard of the tail booms with approximately fifty percent more surface area than original full-scale Pioneer. The larger tail was added to increase elevator power as well as longitudinal stability. The NPS half-scale plane has an elevator proportional to the small tail on the original version of the full-scale Pioneer.

The previous section discussed some of the problems associated with the electrical system before modifications were made. One of the primary reasons for separating the flight control system and the data collection system was to eliminate the possibility of losing control of the aircraft from interference between these to systems. To use the servo as a data collection instrument, it was opened and wire leads were soldered to the small potentiometer inside the servo case. An aileron servo had failed and was replaced after it malfunctioned during ground tests. There was speculation as to whether the failure was caused by

vibration or from the addition of the wires for data collection. Fortunately, the problem was discovered before flight. Figure A.2 shows the schematic for the flight control system.

C. DATA COLLECTION SYSTEM

The new data collection system can be divided into the flight control system instrumentation and the telemetry system. The control-surface potentiometers had to be sensitive to small control deflections and at the same time be resistant to the effects of vibration and noise. The telemetry system allowed the data tape recorder, which was very sensitive to vibration, to be removed from the aircraft and relocated with the ground-based receiver. The entire data collection system was separated into a stand-alone system.

1. Flight Control Instrumentation

The voltage gradient produced by the small internal potentiometers from control-surface deflections was less than one volt for +20° to -20° of movement. The narrow band of voltage from the servos made their data susceptible to vibration and noise from electrical interference. The gearing system adopted with the new potentiometers delivered over four volts for the same range of control surface deflection. Some problems of compatibility with the telemetry system arose for this large range of voltage input and are explained later in Chapter IV.

Individual low-friction one-turn potentiometers were installed to measure the control deflections. Because the ailerons move in equal but opposite directions and the rudders are redundant, only one of each of these controls was instrumented. The elevator was also instrumented. Specifically, these potentiometers measured δ_a, δ_e and δ_r. Figure 3.1 shows the position of the

flight control servos and the data collection potentiometers as they were mounted on the airframe.

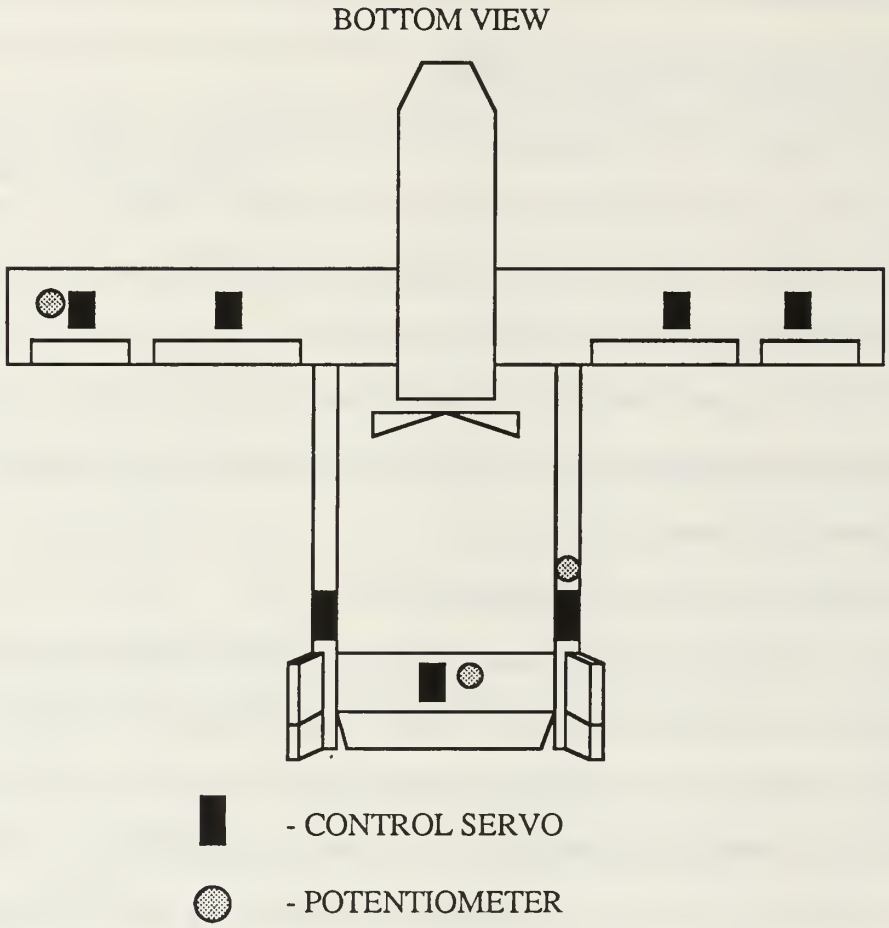

Figure 3.1: Position of Servos and Potentiometers

To use a majority of the deflection range of each potentiometer, gear sets were used to multiply the amount of servo movement. The available potentiometer throw, as seen in Table B.1 of Appendix B, was 330° ± 5°. The control servo output wheel only rotated approximately ± 30° from the control surface neutral position and the actual amount of control surface movement

needed to control flight was substantially less. To increase the amount of potentiometer rotation per unit of control surface deflection, gears were installed to create a ratio of 3.5 to 1. An 84-tooth, 32-pitch, 20°-pressure-angle gear was mounted on a 7/8-inch-diameter servo output wheel for the three desired servos. A similarly-dimensioned 24-tooth gear with integral set screw was used on each corresponding potentiometer.

These particular gears were chosen to strike a balance between creating a suitable ratio (maximizing potentiometer range while minimizing the possibility of control binding) and allowing enough lateral distance between the two units to facilitate mounting. The potentiometers were first mounted on small aluminum plates; then, one plate assembly was mounted next to the right aileron servo on the wing and one next to the servo that controlled the elevator. Figure 3.2 shows how the rudder potentiometer was mounted.

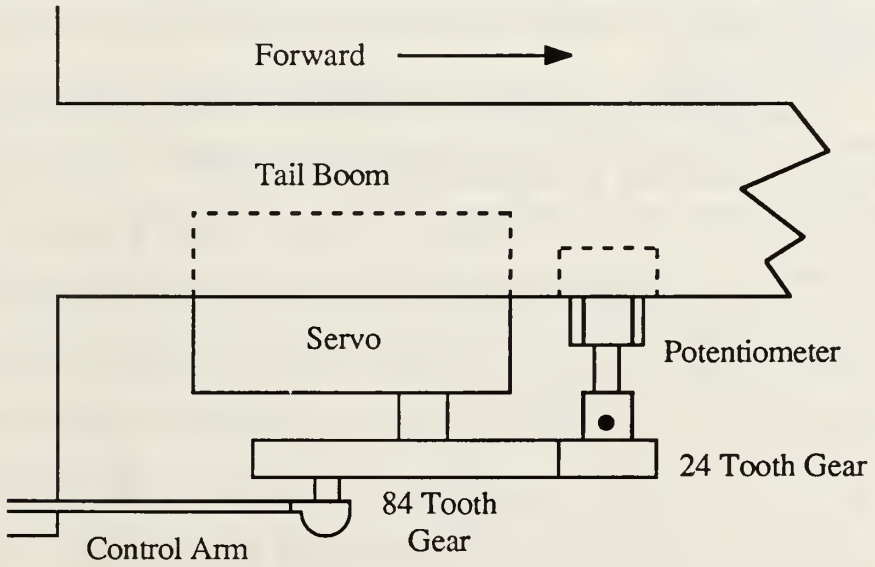

Figure 3.2: Rudder Potentiometer Installation

If desired, the gear ratios could be changed by constructing a new plate for the required post-to-post distance corresponding to the sum of the radii of the two gears. The rudder was a semi-permanent mount in that a single hole was drilled in the left tail boom forward of the servo. If necessary, mounting could be done on the right tail boom. Each potentiometer was mounted with rubber washers on top and bottom of its respective plate to help reduce the effects of vibration. Calibration is discussed in Chapter IV and Figure A.3 shows the schematic for this system.

2. Telemetry System

The previous data collection system used a seven-channel analog tape recorder mounted in the fuselage of the aircraft for recording data output. Vibration, however, prevented the system from functioning properly causing large scatter of the data. A suspension system for the recorder was engineered and tested, but there was no significant reduction in scatter of flight test data [Ref. 10:pp. 15-22].

To eliminate the affects of vibration on data collection, the CHOW-1G telemetry system was developed [Ref. 12:pp. 5-27]. The telemetry system consisted of a seven-channel airborne transmitter and a ground-based receiver. The transmitter gathered the analog inputs from the aircraft potentiometers and the airspeed transducer, converted them to digital signals, then sent them to the ground-based receiver via a seven-pulse serial wave (one pulse per channel). The receiver decoded the digital signals and converted them back to analog output recorded on the original seven-channel tape recorder. The data recorder was now located with the telemetry receiver on the ground where it was no longer subjected to vibration and was able to record the input cleanly.

Two of the problems associated with the original electrical system were excessive demand on the 4.8 Vdc main battery and non-standard input voltage to the data collection potentiometers. The demand on the 4.8 Vdc battery was eased by using the telemetry transmitter's 9.6 Vdc, 500 mAh, NiCd battery as a power supply for the potentiometers, as well as energizing the transmission circuitry. The telemetry transmitter converted the 9.6 Vdc potential to 5 Vdc to power all of the data collection potentiometers which, in turn, standardized the input signal to the data sensors. A complete description of the telemetry system is found in Reference 12 and Figure A.4 shows the diagram for the telemetry transmitter input plug.

D. ALPHA-BETA PROBE

The probe used for measuring α and β consisted of a 17-3/4 inch stainless steel probe shaft with two separate, continuous-turn potentiometers mounted on one end. Brass vanes were mounted on the potentiometers to translate air stream variations to the potentiometer spindles. The probe is pictured in Figure 3.3. The probe mounts to the fuselage by slipping the shaft through a hole in the nose of the aircraft and through a hole in the mounting block approximately five inches aft of the nose. It is secured on the end by a nut and is kept from rotating by a locking pin that slips through a collar on the mounting block and through the shaft. The nut and locking pin are reached through the cockpit access panel.

When mounted, the β potentiometer is the most forward of the two and is located on the top of the probe with the spindle 11-3/8 inches forward of the nose of the aircraft. The α potentiometer is on the starboard side of the probe (looking forward from the cockpit) with the spindle 9-3/8 inches from the nose.

Initially, the vanes were set to zero degrees and the potentiometers were synchronized so that approximately 2.5 Vdc output marked the center position.

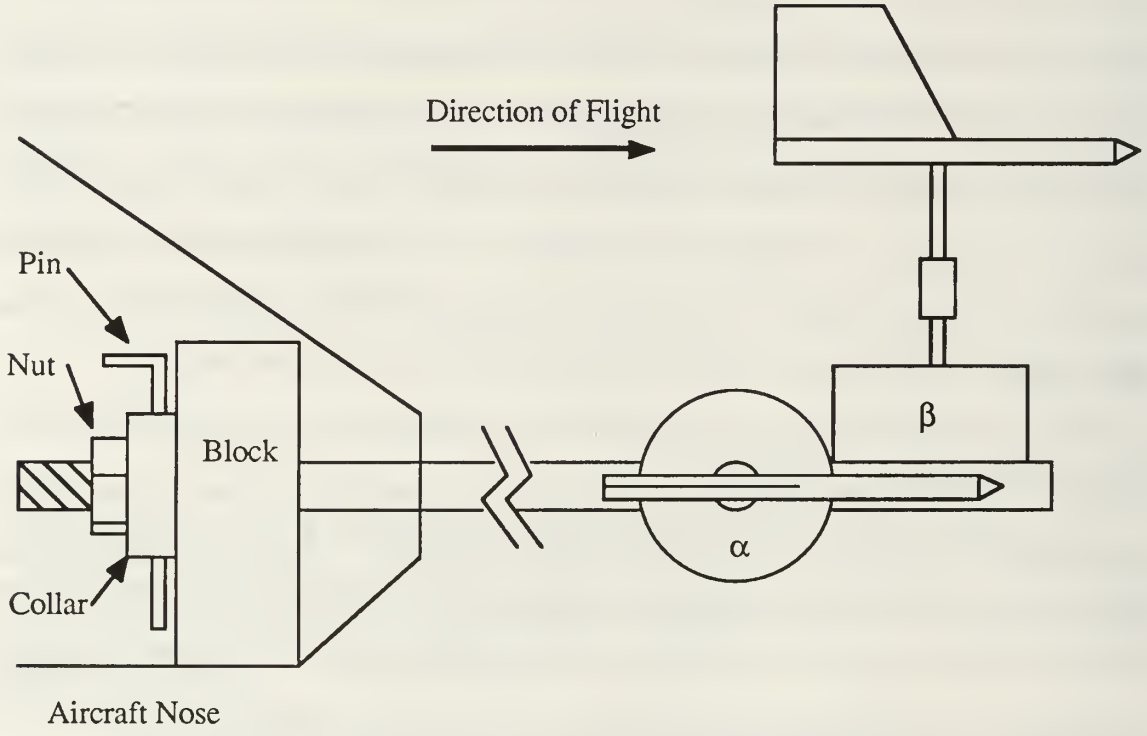

Figure 3.3: α-β probe

This base setting provided the greatest range of voltage output available for measurements and correlated with the neutral settings of the control surface potentiometers. Calibration was done using a specially designed calibration tool consisting of a rod and protractor that attached to the probe shaft and is explained further in Chapter IV. The electrical diagram for this system is provided in Figure A.5.

E. AIRSPEED INDICATOR

Airspeeds were measured with a pressure transducer and signal-conditioning unit designed to provide linear voltage output with changes in indicated airspeed. The useable range of the unit was designed by the manufacturer to be 30 to 130 KIAS. The 4.8 Vdc main battery provide power to the dc to dc converter which supplied the ±15 Vdc used by the airspeed unit. To measure output voltage, wires from the IAS signal output channel (pin six) and the signal return channel (pin seven) were connected to the telemetry transmitter input plug wiper and ground pins, respectively. The case ground (pin nine) was connected externally to the signal return lead as recommended by the manufacturer to reduce noise during testing and use.

The airspeed indicator was designed to provide a signal gradient of 75 mVdc per KIAS. Since 5 Vdc was the maximum design input voltage for the telemetry transmitter, it was expected (before calibration) that airspeed would need to be limited to a maximum of approximately 75 KIAS to avoid over-voltage of the transmitter. As with the potentiometers, some compatibility problems arose with voltage output from the pressure transducer and input to the telemetry transmitter. Calibration is explained further in Chapter IV. The schematic for the airspeed system is shown in Figure A.6 and a table of the airspeed unit's specifications is given in Appendix B.

F. DATA REDUCTION SYSTEM

After receiving the signal generated by the telemetry transmitter during flight test maneuvers, the ground-based receiver converted the seven-pulse serial wave back to analog form for recording on a magnetic tape cassette. Next, the

data were processed by playing the tape in a seven-channel bench playback unit, converted once again through an A-D converter to digital form and input to an AT-type personal computer. The data were stored on the hard disk for permanent record and to allow processing at a later date. The data were reduced using "LabTech Notebook" software and histograms were plotted using a locally-developed FORTRAN code called REDUCE [Ref. 12:pp. 44-50].

IV. EXPERIMENTAL PROCEDURES

A. CALIBRATION

Before flight testing could be conducted, the data collection, α-β, and airspeed systems had to be calibrated. The relationships between displacement angles and velocities with voltage outputs from the various sensors needed to be established. The calibration procedures in this section were performed several times to determine their repeatability. The data for the calibration checks are compiled in Appendix C.

1. Flight Controls Calibration

The data collection potentiometers mounted at the flight control surfaces were first calibrated without the telemetry transmitter installed in the aircraft. A direct current power source was used to generate 5 Vdc to simulate the telemetry unit's power output to the potentiometers. A volt meter was connected to the potentiometer output leads to measure the voltage changes produced when the control surfaces were moved.

To set the flight control surfaces to their zero displacement (or neutral) position, the flight control servos were energized and set to their neutral, zero-trim positions. Then, each control linkage was adjusted until all of the control surfaces were neutral. Next, the set screws on the potentiometer gears were loosened and the potentiometers were adjusted to set a voltage output of approximately 2.5 Vdc. This setting was roughly in the center of the potentiometer's rotation range, allowing equal amounts of rotation in either direction of control servo movement.

The rudder was calibrated using the tool shown in Figure 4.1. The protractor was marked in five-degree increments and was aligned so the center point was on the rudder hinge axis. With the rudder set to its neutral position, the trailing edge aligned with the zero degree mark and the output voltage was recorded. The rudder was then displaced in five-degree increments in each direction and those output voltages were recorded, as well. The data are listed in Table C.1 and a plot of rudder deflection versus voltage is shown in Figure 4.2. The output from the calibration was well within the bounds of a linear curve-fit which could be used for future calibration and data reduction.

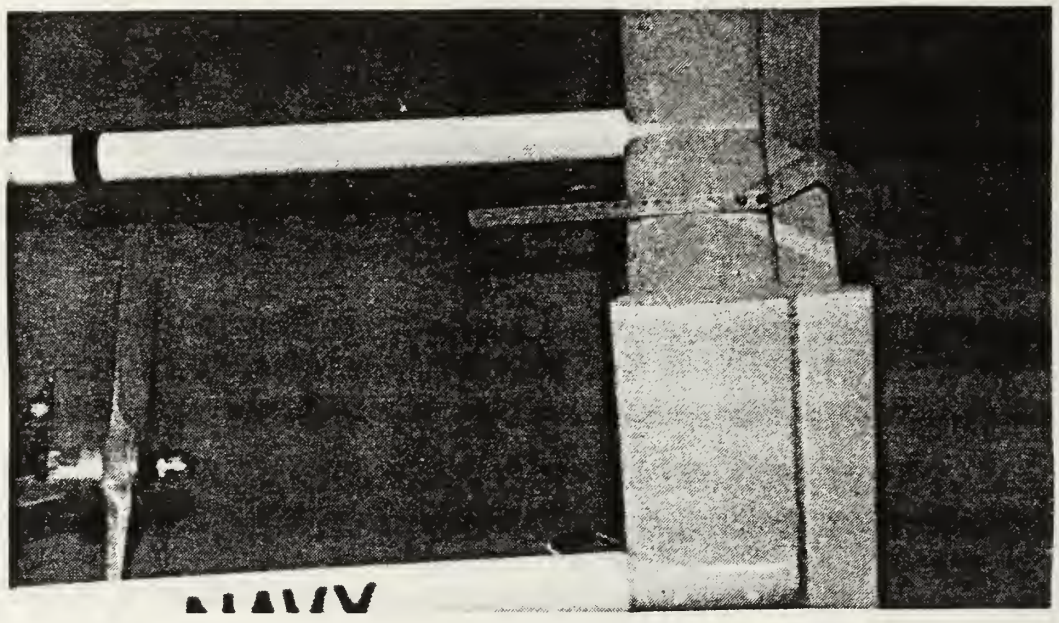

Figure 4.1: Rudder and Elevator Calibration Tool

The elevator was calibrated using the same procedures and the same calibration tool. The results of the calibration are plotted in Figure 4.3 and the data are also compiled in Table C.1.

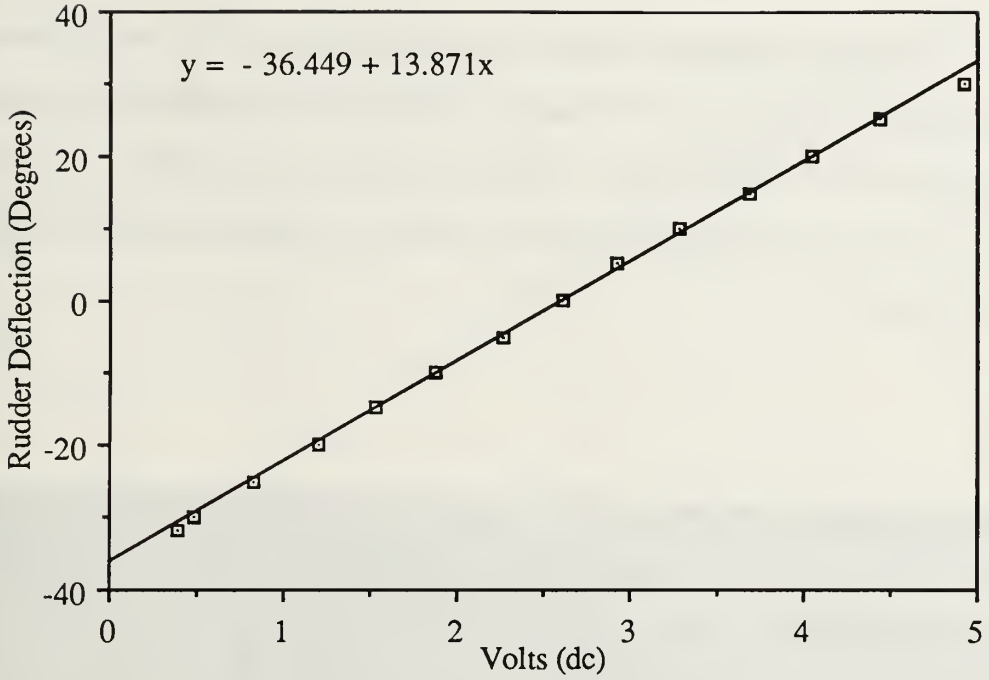

Figure 4.2: Rudder Calibration Curve

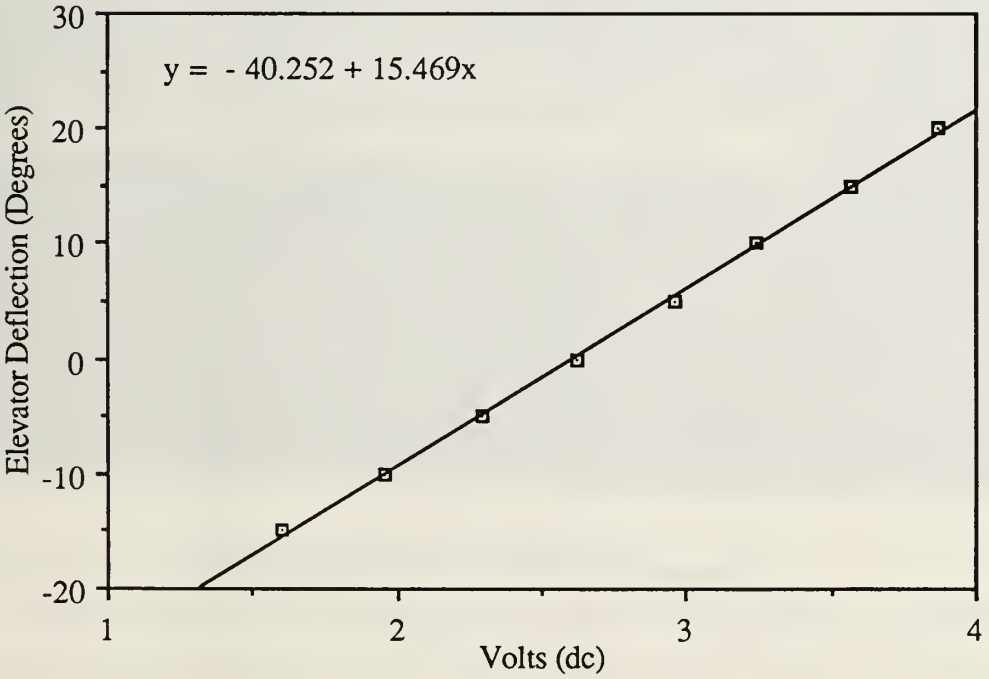

Figure 4.3: Elevator Calibration Curve

The same procedures used for calibrating the other control surfaces were repeated for the aileron. However, a larger radius protractor was needed for the larger aileron chord length. The tool used for this calibration is pictured in Figure 4.4. The calibration curve is plotted in Figure 4.5 and the data are listed in Table C.1.

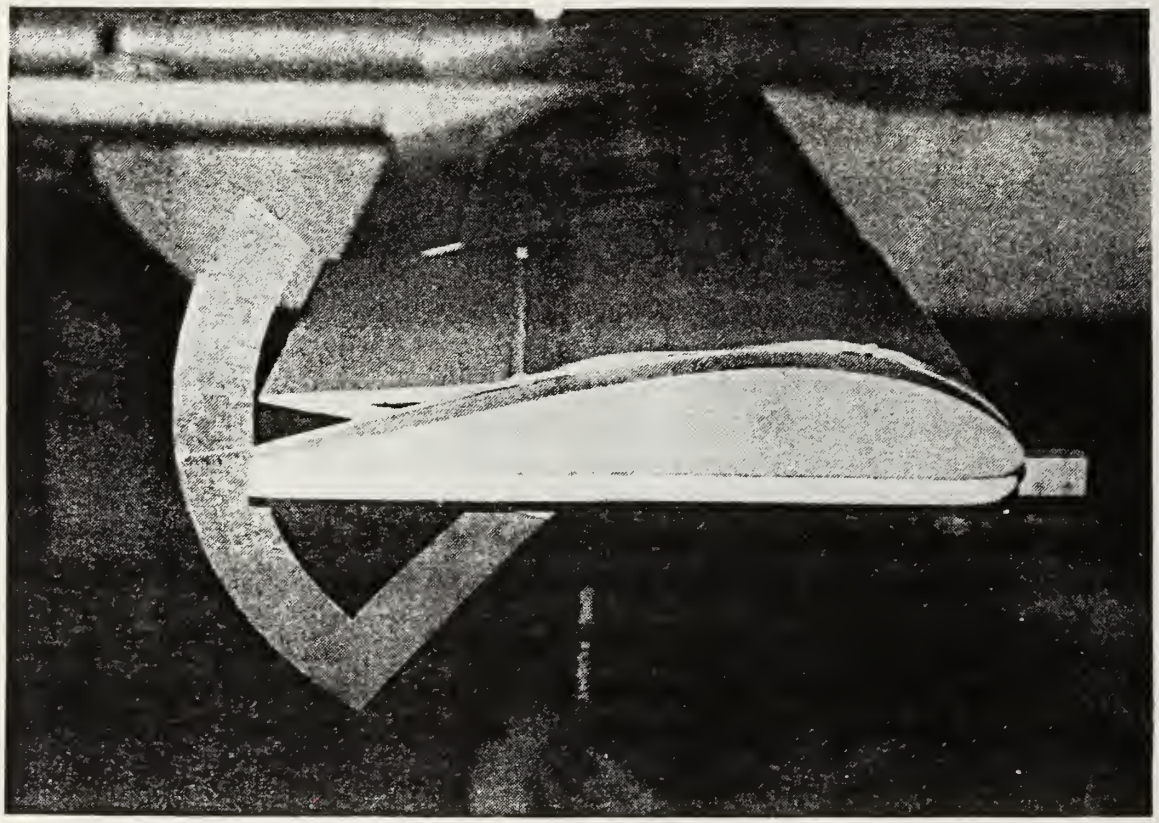

Figure 4.4: Aileron Calibration Tool

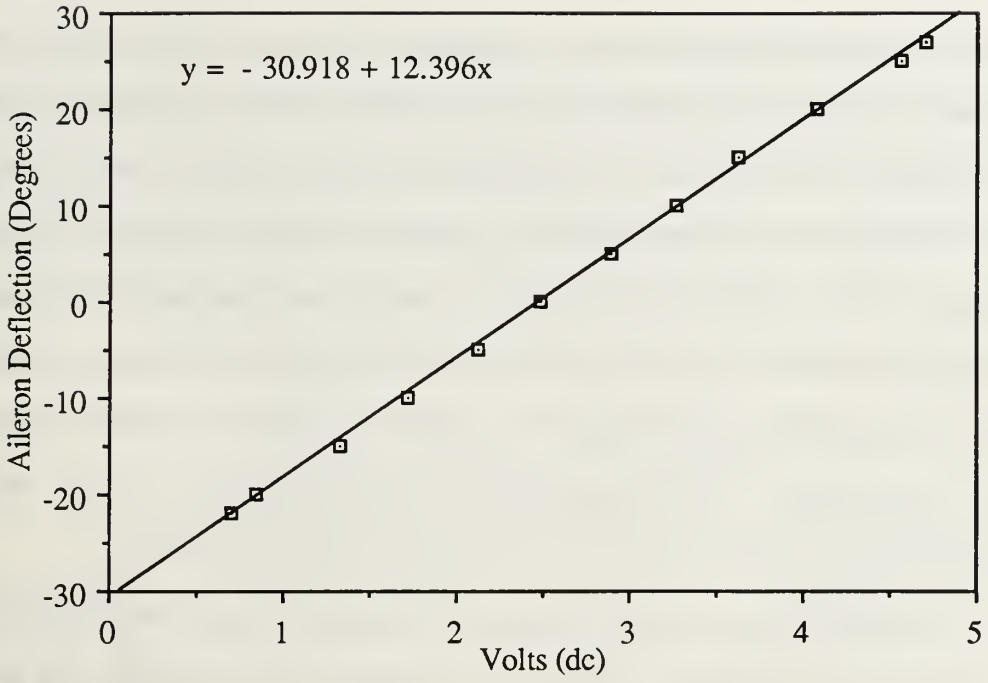

Figure 4.5: Aileron Calibration Curve

2. Telemetry Transmitter Calibration

The telemetry transmitter was installed in the aircraft and the control surfaces were recalibrated. The transmitter was designed to receive a maximum input voltage of approximately 5 Vdc. The encoder portion of the transmitter produced a seven pulse signal train (one pulse per output channel) having a width of 1.0 ± 0.5 ms per pulse. Any voltage inputs corresponding to that which would produce less than a 0.5 ms pulse would be lost and those voltage inputs producing a pulse width greater than 1.5 ms would also be lost along with any other signal that followed it in the pulse series.

The manner in which the potentiometers were initially set in sub-section one drove the pulse widths off the low end of the scale but failed to reach the 1.5 ms pulse width upper limit when the controls were deflected. To adjust the pulse

width, the control surfaces were displaced fully to produce low voltage outputs. The potentiometers were adjusted until 0.5 ms pulse widths were produced. The control surface potentiometers were adjusted to produce the low end of the pulse width scale because trim potentiometers in the transmitter could adjust only the upper limit of the pulse width. When the control surfaces were deflected to drive the pulse widths to the low end of the threshold, the 0.5 ms pulse was produced. But, reversing the controls caused them to bind after only a few degrees of movement. The potentiometers had been skewed so far to the high end of their output range (close to 5 Vdc) that rotation was halted.

The trim potentiometers within the telemetry transmitter were adjusted but full deflections of the controls were not possible. Also, the encoder still did not receive an acceptable range of voltage. The pulse widths were driven off the upper or lower thresholds, or both, depending on the combination of control surface potentiometer and transmitter trim potentiometer settings. Upon further investigation, it was determined that the acceptable range of voltage input that the encoder could use for producing the proper pulse width was about 3.7 Vdc to 5.0 Vdc. The trim potentiometers were adjusted through their full range but only succeeded in shifting this maximum acceptable 2.3 Vdc window between the extremes of the control surface potentiometer's zero to five volt output range. In other words, the maximum useable 2.3 Vdc encoder window could not be expanded by adjusting the trim potentiometers or the control surface potentiometers.

To alleviate the problems of control binding and out of range pulse widths, the gear sets were removed and control arms were installed. The control arms produced a 1:1 ratio between servo movement and data collection

potentiometer movement. This conversion greatly decreased the resolution of the control surface potentiometer output but allowed the transmitter to be tuned to an acceptable range of pulse widths for the full deflection of the control surfaces. The system was readjusted and recalibrated so that full deflections produced pulse widths inside the 1.0 ± 0.5 ms window. The results of this calibration are plotted in Figure 4.6 and the data are given in Table C.2. Reference 12 has a detailed discussion on calibrating the telemetry transmitter.

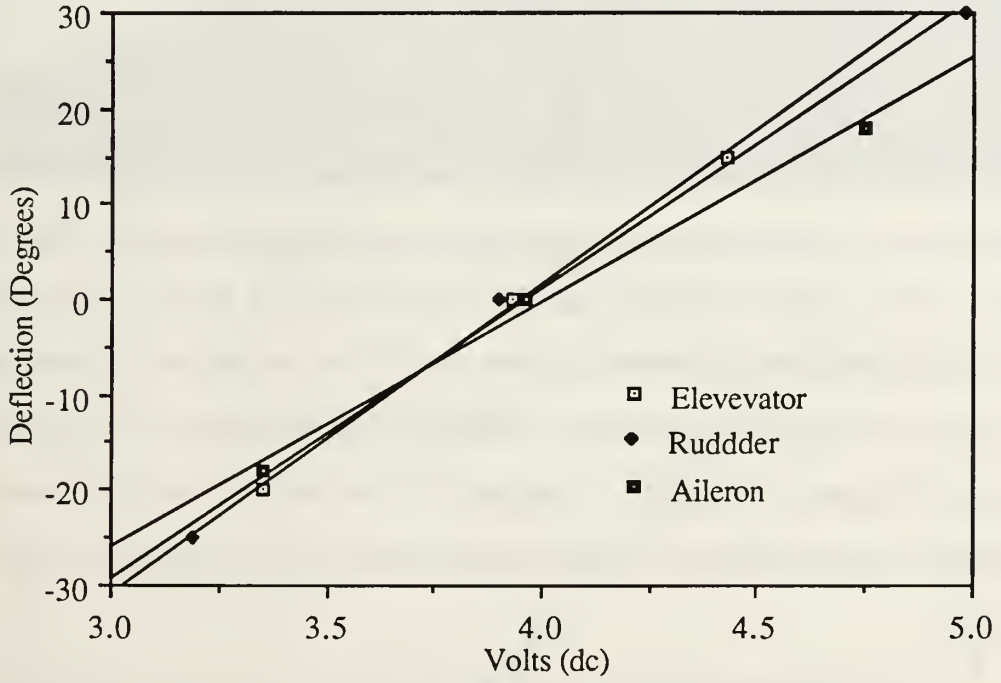

Figure 4.6: Control surface Calibration with Control Arms Installed

Figure 4.6 clearly shows the differences in resolution between the output of the potentiometers when using the control arms and when using the gear sets . The steeper slopes of the control arm outputs show that much greater control deflections produced much smaller voltage changes. The curves were

skewed to the right due to adjustments of the transmitter trim potentiometers. The position of the curves could be skewed left or right by adjusting the transmitter and control surface potentiometers but the slopes could not be changed. The curve for the aileron was slightly shallower than the other curves because a special output wheel and arm arrangement was adapted to provide slightly greater than 1:1 rotation ratios. Modifications to the telemetry transmitter data-input circuit are being considered to make use of the wider voltage range available with the gear sets.

3. α-β Calibration

The α-β potentiometers were calibrated in the same manner as the control surfaces. The protractor pictured in Figure 4.7 was aligned with each potentiometer so that the vane was parallel with the probe shaft. The voltage output at this position represented the zero deflection point. The vane was rotated from the zero deflection point to +45° in five degree increments and repeated in the opposite direction. The data are recorded in Table C.3 and plotted in Figures 4.8 and 4.9. The probe vanes worked well for comparison purposes , but no in-flight or installed calibration of the α-β probe has yet been conducted.

The α-β potentiometers used brass vanes to sense the direction of the on-coming air flow and there was no other type of mechanical interface. For this reason, no ratio of input signal to output signal existed as with the flight control potentiometers. The telemetry transmitter always received a one to one signal from the probe. There was no need to recalibrate the α-β system to the telemetry system's voltage range. The only consequence of the reduced input range to the transmitter was a decrease in the useable range of α and β.

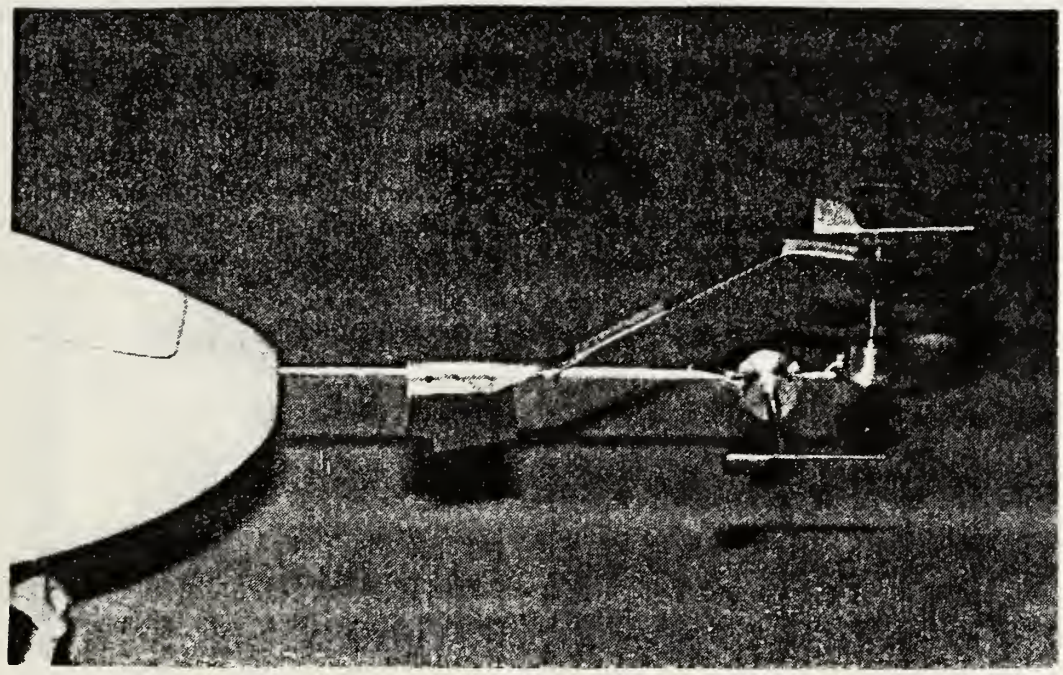

Figure 4.7: α-β Calibration Tool

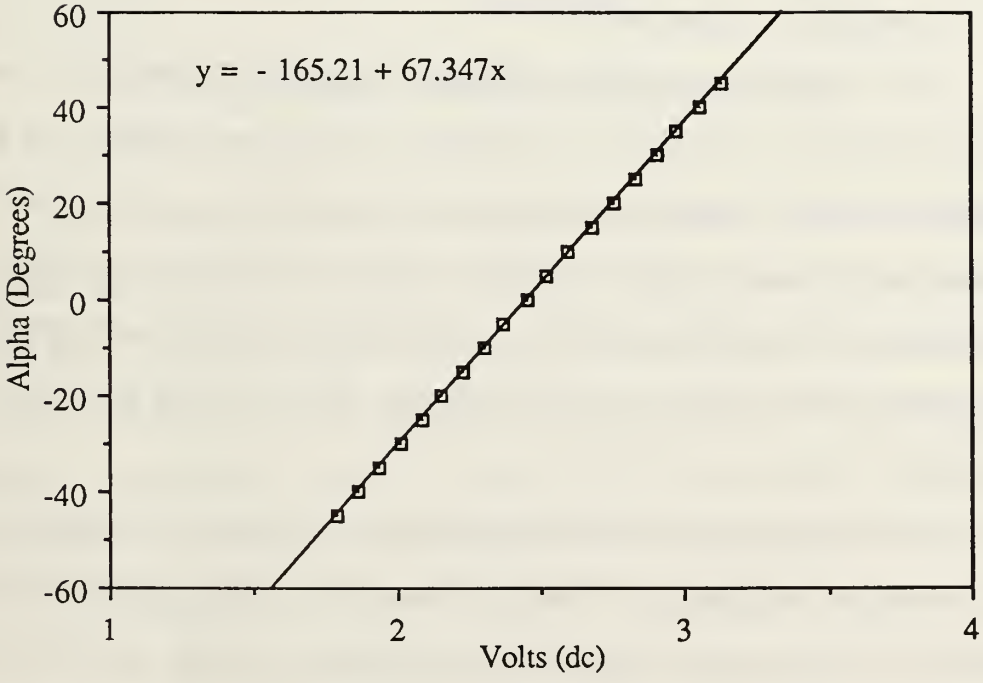

Figure 4.8: Angle of Attack Calibration Curve

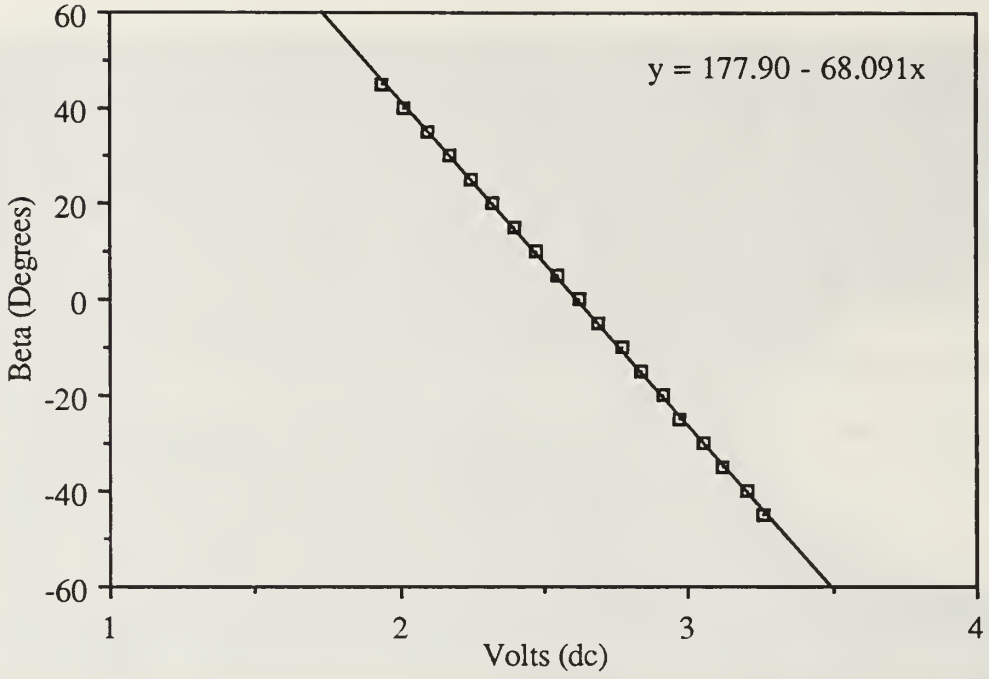

Figure 4.9: Side Slip Angle Calibration Curve

4. Airspeed Calibration

The airspeed unit was calibrated using the "Schmidter" pressure calibration device. The device combined a U-tube manometer and a hand cranked piston that created and held a constant pressure. The manometer measured the change in pressure (ΔP) in inches of water (cm of H_2O). The pressure line from the "Schmidter" was connected to the total pressure port (P_T) of the airspeed unit while the static pressure port (P_S) was left open to the atmosphere.

The airspeed unit converted the pressure change to a voltage output and a plot of airspeed and voltage is shown in Figure 4.10. The relationship between airspeed and voltage was not linear, but the equation for the curve fit could be used to calculate values of airspeed from volts. Also, the unit produced

approximately 1.8 Vdc at zero airspeed. The calibration data for the airspeed transducer are compiled in Table C.4, of Appendix C.

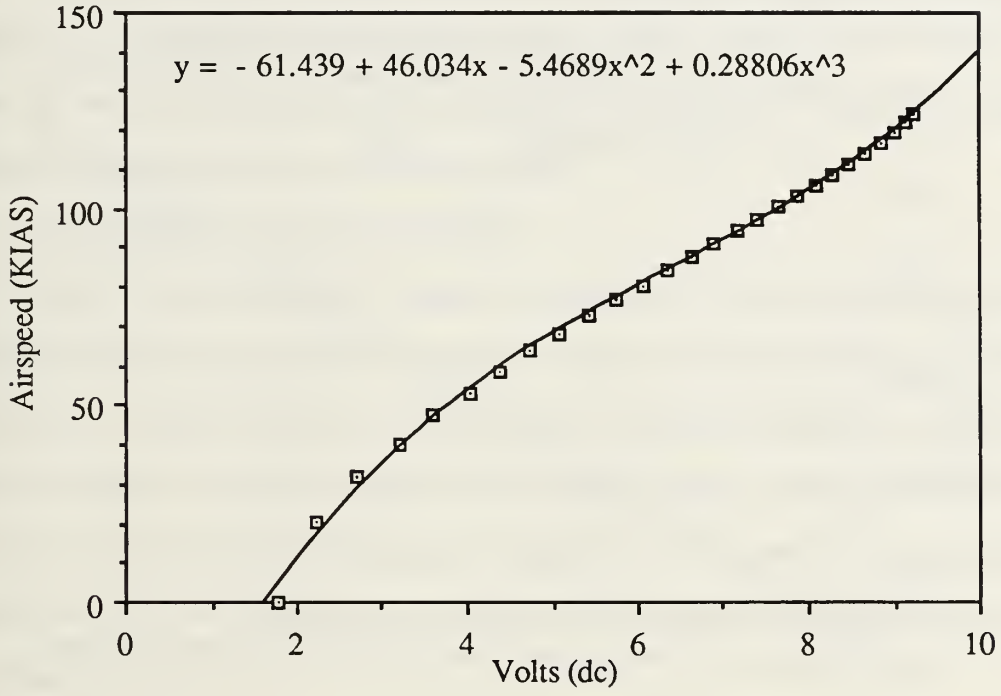

Figure 4.10: Airspeed Calibration curve

The same problem of voltage compatibility with the telemetry transmitter experienced by the data collection potentiometers also affected the airspeed unit. The same range of output voltage was used by the transmitter for measuring indicated airspeed. The airspeed trim potentiometer in the telemetry transmitter was adjusted so the 0.5 ms pulse width corresponded to ΔP=4.2 cm of H_2O and the 1.5 ms upper limit of pulse width corresponded to ΔP=12.0 cm of H_2O. These pressure differences converted to an airspeed range of 50 to 85 KIAS which is the most useable range of flight velocities for the half-scale Pioneer. An examination of Figure 4.10 shows that this airspeed range falls on a

portion of the original calibration curve that is fairly linear. A plot of the new local calibration curve is shown in Figure 4.11. This curve was used with the data reduction computer software to calibrate the flight data.

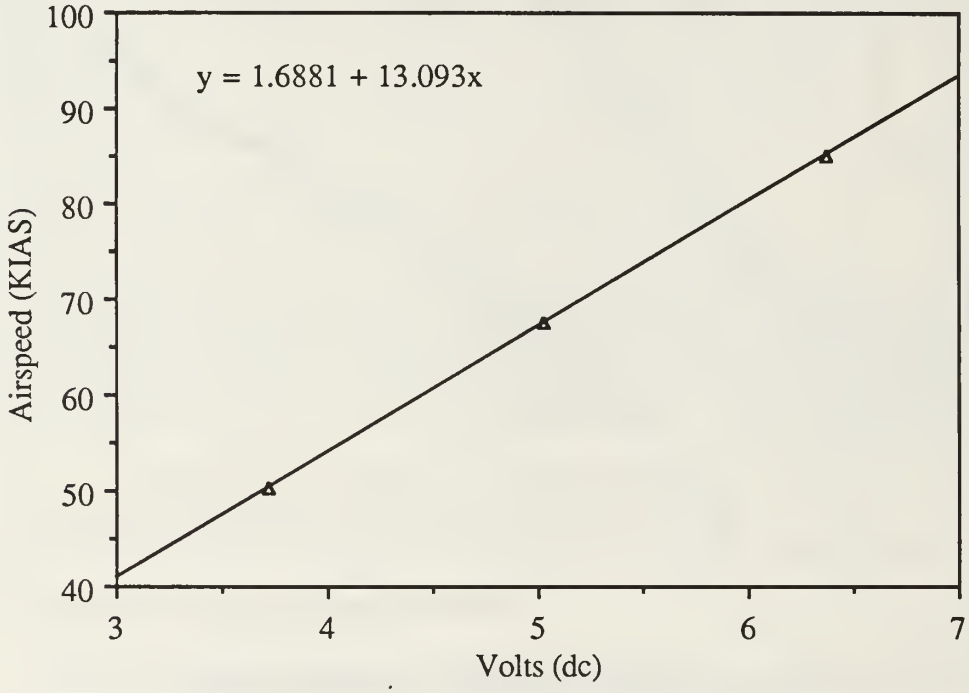

Figure 4.11: Airspeed Calibration Curve with the Telemetry Transmitter

B. STATIC STABILITY

Aircraft static stability is defined as the initial tendency of an aircraft to return to an equilibrium condition once it has been disturbed from that steady state. Equilibrium is the state of an aircraft where all of the forces and moments acting on it are balanced. If the aircraft has an initial tendency to return to the original equilibrium condition from which it was disturbed, it is said to have positive static stability (statically stable). If the aircraft initially tends to diverge

further away from the equilibrium position after it has been disturbed, it is said to have negative static stability (statically unstable). If there is no tendency to move in either direction, the aircraft has neutral static stability. The static stability of an aircraft only characterizes these initial tendencies of movement toward or away from equilibrium and gives no information about the handling qualities of the aircraft over a period of time.

1. Longitudinal Static Stability

From the definition above, an aircraft would exhibit positive longitudinal static stability if it tended to return to trimmed flight conditions (equilibrium) when disturbed in pitch. If a nose-up displacement occurred (positive increase in α), the stable aircraft would develop a nose-down pitching moment (a positive pitch moment, by definition). Likewise, if a nose-down displacement occurred (decrease in α), the stable aircraft would develop a nose-up pitching moment.

Another way of expressing these tendencies is to plot C_M versus α. If the slope of the curve is positive, the aircraft would be unstable; a horizontal line would represent neutral static stability, and a negative slope would indicate positive static stability. The slope of the moment coefficient curve can be written as $dC_M/d\alpha$, dC_M/dC_L, or simply C_{M_α}.

In determining the longitudinal static stability characteristics of an aircraft, the moments are summed about the center of gravity. The resulting equation can be reduced to the non-dimensionalized form shown in Equation 4.1:

$$C_M = C_{M_{owb}} + \left(h - h_o\right) C_L - \frac{l_t S_t}{\bar{c} S} C_{L_t} \qquad (4.1)$$

where $l_t S_t / \bar{c} S = \overline{V}$ (tail volume ratio) and is assumed to be constant. Also, h_o is assumed to be constant for subsonic speeds. Differentiating Equation 4.1 with respect to C_L gives Equation 4.2.

$$\frac{dC_M}{dC_L} = \left(h - h_o\right) - \overline{V}\frac{dC_{L_t}}{dC_L} \tag{4.2}$$

Longitudinal stability is therefore a function of the location of the center of gravity (h) and the rate of change in the tail lift with changes in wing lift. If the center of gravity is forward of the aerodynamic center such that $h-h_o<0$, a stabilizing effect is created. Recall that the more negative C_{M_α} is, the more stable the aircraft is, by definition (this characteristic may not necessarily be desirable). As h is moved aft of the aerodynamic center such that $h-h_o>0$ there is a destabilizing effect (C_{M_α} becomes less negative). When the two terms on the right hand side of Equation 4.2 are equal, the slope becomes zero and the aircraft exhibits neutral static stability. This critical position of h is also described as the neutral point of the aircraft and any further aft movement of h will cause the aircraft to become unstable.

To determine the neutral point of the aircraft using flight test methods it would be necessary to determine C_M for the aircraft. This calculation can be done indirectly using the moment coefficient due to the displacement of the elevator (which is equal and opposite to that for the entire aircraft) required to maintain new equilibrium flight conditions. Equation 4.3 shows the relationship.

$$C_{M_{cg}} = -\overline{V} C_{Lt_{\delta e}} \Delta\delta_e \tag{4.3}$$

Differentiating Equation 4.3 with respect to C_L yields Equation 4.4 for longitudinal stability as a function of elevator deflection and lift coefficient.

$$\frac{dC_M}{dC_L} = - \overline{V} C_{Lt_{\delta e}} \left(\frac{d\delta_e}{dC_L} \right) \tag{4.4}$$

Plotting changes in δ_e versus changes in C_L produced linear curves with different slopes for each center of gravity position. By plotting the slopes of these lines ($d\delta_e/dC_L$) against their respective center of gravity position, it was possible to extrapolate to the value for zero slope, giving the neutral point. This characteristic is a function of elevator displacement and not of the forces that were generated by the deflections and is termed the stick fixed neutral point [Ref. 13:pp. 4.3-4.9]. As the flight-control system is irreversible, there is no stick-free neutral point.

2. Directional Static Stability

Directional static stability is commonly referred to as "weathercock" stability, and the greatest contributor to directional stability are the vertical stabilizers. The fuselage can also be a large contributor to the directional stability of an aircraft. Other factors, such as wing sweepback, influence directional stability but are either not applicable to the Pioneer or are insignificant compared to the influence of the vertical stabilizers. Directional stability is actually a measure of the aircraft's sensitivity to β. An aircraft is said to exhibit positive directional static stability if β generates a yaw moment which acts to restore the nose of the aircraft into the relative wind (reducing the magnitude of β toward zero) [Ref. 13:p. 7.1].

The consequence of having a misalignment with the relative wind, which creates β, is that a yawing moment is produced. A positive yawing moment coefficient (C_N) is defined as a clockwise rotational moment. Positive β is defined as the relative wind being aligned on the right side of the nose (wind in the right ear). When C_N is plotted against β, ideally, a straight line through the origin is produced. The slope of this line is $dC_N/d\beta = C_{N\beta}$ and is positive for positive directional stability. That is, for $+\beta$, a $+C_N$ is produced which tends to weathercock the fuselage into the relative wind in a stabilizing manner ($+C_{N\beta}$).

To determine the directional stability characteristic of the Pioneer, the steady heading side slip flight test was performed. This test was similar to the longitudinal stability flight test in that it measured the moments necessary to hold the aircraft away from the trimmed flight condition. It was necessary to use rudder deflection to generate β coupled with aileron deflection to produce bank angle (ϕ) to keep a steady heading. This is commonly known as the wing-down, top-rudder technique often used for cross wind landings. In this way, the side force and moment generated by β are countered by the forces and moments created by the rudders and ailerons.

The side force stability derivative ($C_{Y\beta}$) is expressed in terms of the side force control derivatives ($C_{Y\delta_r}$ and $C_{Y\delta_a}$) in Equation 4.5.

$$C_{Y_\beta} = - C_{Y_{\delta r}} \frac{d\delta_r}{d\beta} - C_{Y_{\delta a}} \frac{d\delta_a}{d\beta} - C_L \frac{d\phi}{d\beta} \qquad (4.5)$$

Equation 4.6 shows the lateral stability derivative ($C_{l\beta}$) in a similar expression; however, rolling moment is not dependant on angle of bank (ϕ).

$$C_{l_\beta} = - C_{l_{\delta r}} \frac{d\delta_r}{d\beta} - C_{l_{\delta a}} \frac{d\delta_a}{d\beta} \tag{4.6}$$

Lastly, Equation 4.7 shows the yawing moment stability derivative (C_{N_β}) expressed as a function of the control surface deflections.

$$C_{N_\beta} = - C_{N_{\delta r}} \frac{d\delta_r}{d\beta} - C_{N_{\delta a}} \frac{d\delta_a}{d\beta} \tag{4.7}$$

Reference 13 states that the control derivatives are essentially constant and can be estimated using using wind tunnel tests or through empirical methods such as Datcom. Lyons determined some of these values using the low order computer panel method PMARC [Ref. 9:pp. 33-40]. From steady heading side slip flight testing, linear plots can be made to determine $d\delta_r/d\beta$, $d\delta_a/d\beta$, and $d\phi/d\beta$. If all the variables on the right hand side of each of the above equations are known, the stability derivatives can be calculated. Using manufacturer supplied data from Reference 10, the calculated values for $d\delta_r/d\beta$ and $d\delta_a/d\beta$ were compared to the measured values extracted from flight test data. Again, since this flight test involved measuring the displacements of each of the control surfaces and not the forces associated with them, the results were a measure of the stick fixed directional stability.

V. RESULTS

A. LONGITUDINAL STABILITY

The center of gravity (cg) position for the basic aircraft with no fuel was determined to be 36.6% MAC (MAC=11.85 inches). By adding ballast to the nose section of the aircraft, the cg could be manipulated, and the weights necessary to place the cg at 30.0%, 33.4%, and 36.1% were determined. Four data collection runs were made during flight testing for each cg position. The first run was made at full power to achieve the fastest indicated airspeed. Each successive pass was made at slower airspeeds until the final pass was performed at the minimum airspeed, as dictated by the pilot. The data collection runs were commenced with the aircraft set in straight and level flight and stabilized at the desired airspeed.

The data were extracted from the data recorder tape and reduced to plot Figures 5.1, 5.2, and 5.3 and are compiled in Table D.1 of Appendix D (the * indicates airspeed was extrapolated). Each line in the figures represent one of the cg positions and each point on a particular line represents one of the four data runs for that particular cg. Only two passes were made with the cg in the aft position due to a perceived in-flight interference problem in the flight control system.

Two characteristics are readily discernable from these three figures. First, the forward-cg curve in Figure 5.1 is more shallow than the curve in Figure 5.2. This result appears unrealistic, in that the 30.0% cg would have been less stable than the 33.4% cg location. By the discussion in Chapter IV, the forward-cg

would have to have been closer to the neutral point than the mid-cg; a physical impossibility, unless the aircraft were unstable, in which case the slopes of these curves would have been negative reciprocals of the values presented.

The second interesting characteristic of the figures above is that the aft-cg curve in Figure 5.3 has a positive value for its slope. This would indicate that the aft-cg was located behind the neutral point causing the aircraft to be unstable. This condition would have been extremely difficult for the pilot to control, requiring, in some instances, reverse controls inputs to achieve normal flight operations.

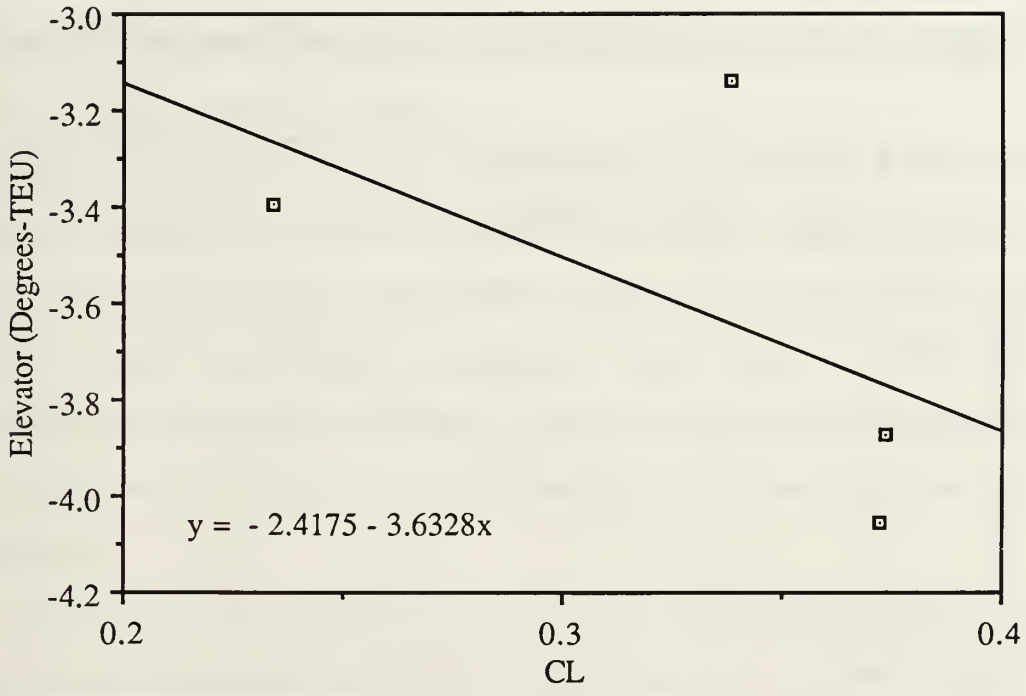

Figure 5.1: Elevator Deflection versus Lift Coefficient for 30.0% cg

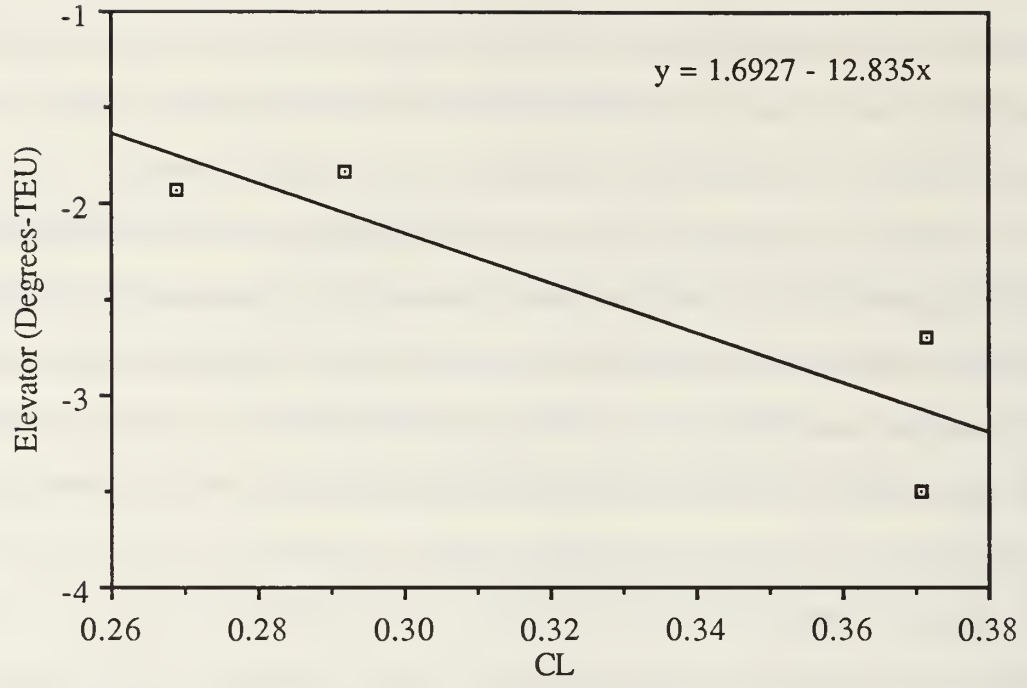

Figure 5.2: Elevator deflection versus Lift Coefficient for 33.4% cg

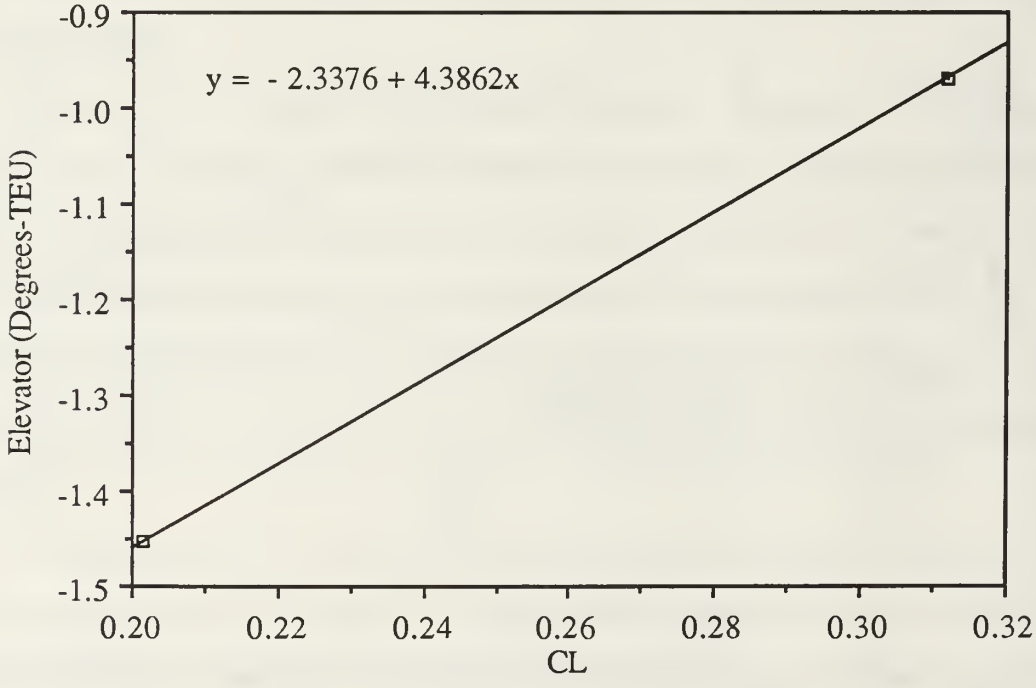

Figure 5.3: Elevator deflection versus Lift Coefficient for 36.1% cg

Anderson outlines a method for theoretically determining the neutral point of an aircraft by estimating $C_{M\alpha}$, and using the center of gravity and the lift curve slopes of the wing and tail. Using this method, $C_{M\alpha}$ for the half-scale Pioneer was calculated to be -0.63, indicating a stable aircraft. The neutral point was calculated using Equation 5.1. The theoretical value for h_n using this method is 47% MAC. [Ref. 14:pp. 384-388]

$$C_{M_\alpha} = C_{L_\alpha}(h - h_n) \tag{5.1}$$

Lyons used computational methods to predict $C_{M\alpha}$ for the small-tail version of the full-scale Pioneer. The value he computed was -0.756. Again, this value indicated that the aircraft was inherently stable. He computed the neutral point to be 51% MAC. [Ref. 9:PP. 25-28]

The slope of each of the curves from Figures 5.1, 5.2, and 5.3 was plotted against the cg position at which the data was collected. Figure 5.4 shows the results. The unreasonable characteristics apparent in the first three figures showed as scattered data in the figure below. Since a curve could not be fit to the data with any reasonable accuracy, the theoretical and computational values for the neutral point location were plotted along with the flight test data for comparison.

The data on the previous figures shows that trim changes resulted in small amounts of elevator deflection changes, usually less then a degree. Because the deflections are so small, the gear sets should be reinstalled on the elevator to improve the resolution, and the runs repeated. With the small deflections, the telemetry signal pulse width should not be driven out of range.

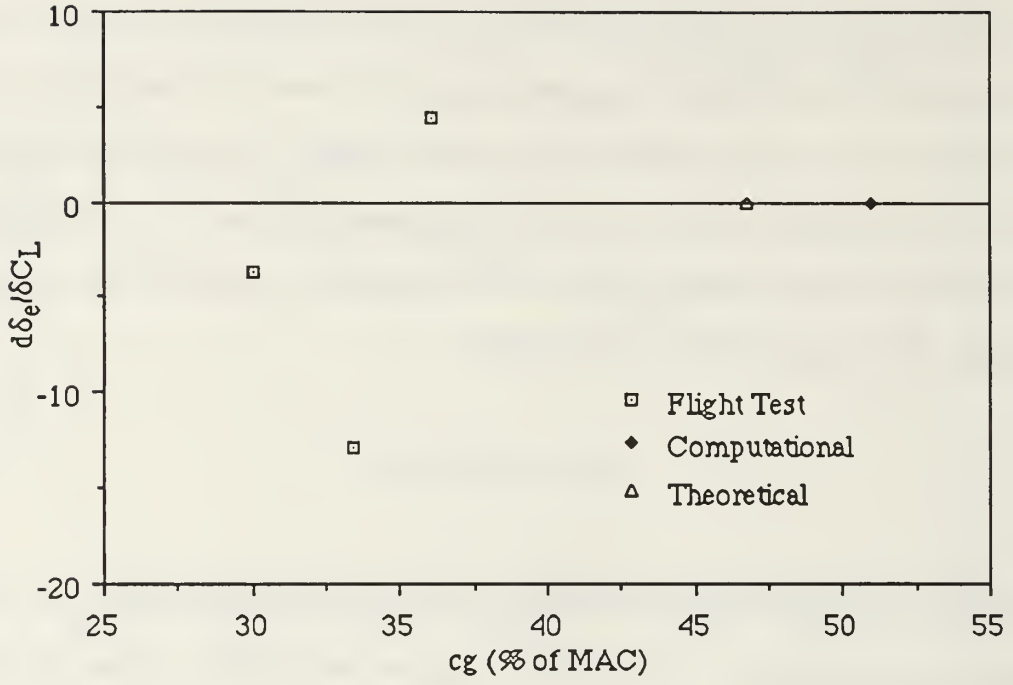

Figure 5.4: Elevator Deflection Curve Slope versus cg Position

The pilot commented, after flight testing, that each cg position was comfortable and controllable. The forward cg created a slightly sluggish feel but no unreasonable effort was required to fly any of these cg positions. The aircraft was flown once with the cg positioned at 40.3% MAC. The pilot commented that the aircraft was extremely sensitive to control inputs and was very difficult to fly.

B. DIRECTIONAL STABILITY

Directional stability was characterized using steady heading side slip flight maneuvers. Five data collection runs were made with the aircraft in the clean configuration (flaps retracted) and the cg at 33.4% MAC. The values of δ_r and δ_a are plotted against β in Figures 5.5 and 5.6, respectively, and the data are tabulated in Appendix D, Table D.2.

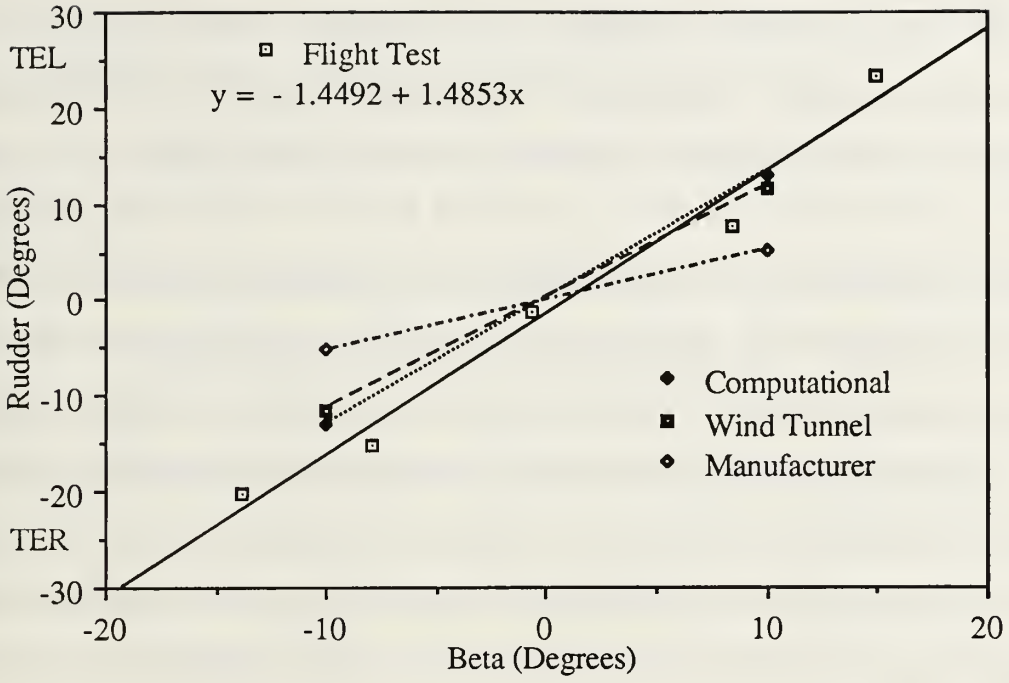

Figure 5.5: Rudder Deflection Versus Side Slip Angle

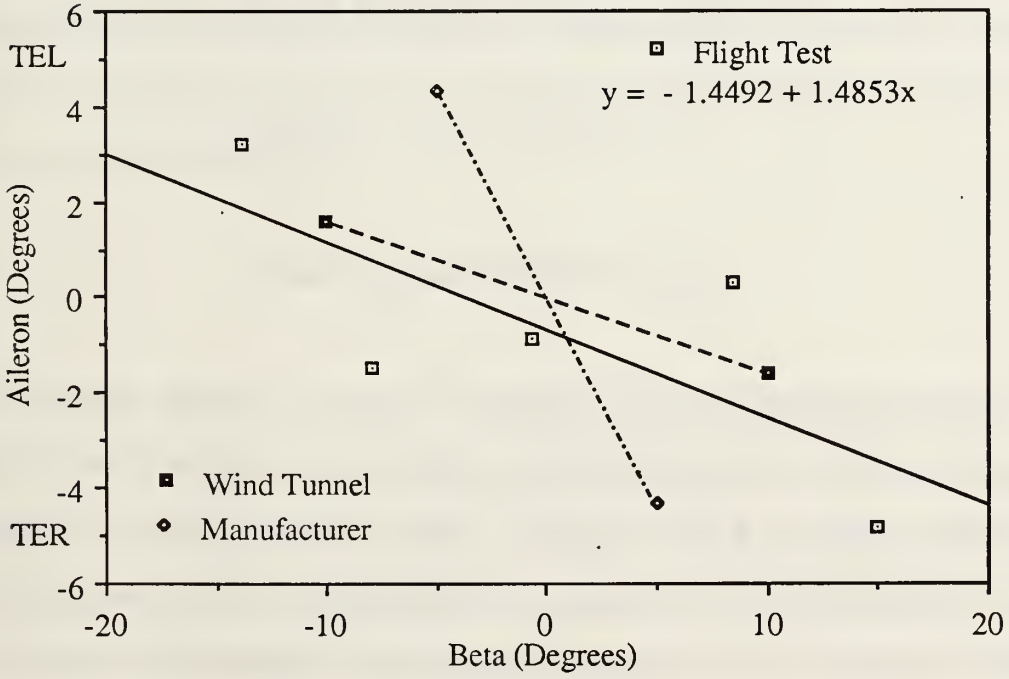

Figure 5.6: Aileron Deflection Versus Side Slip Angle

The first two passes were made with left rudder inputs to create $+\beta$. The first pass was made with approximately half left rudder deflection and an appropriate amount of right aileron to keep the aircraft tracking on a steady heading. The second pass was made with full left rudder with an increased amount of right aileron to track straight. The third pass was made straight and level in trimmed flight and the last two passes were performed with control inputs opposite of the first two runs. Each pass was made at a medium speed.

Although it is difficult to quantify desirable directional stability, the curves constructed from flight test data in Figures 5.5 and 5.6 were compared with other sources of data to characterize this stability parameter. The linear system of equations for equilibrium of the Pioneer is shown in Equations 5.2, 5.3, and 5.4.

$$- C_L \sin(\phi) = C_{Y_\beta} \beta + C_{Y_{\delta r}} \delta_r + C_{Y_{\delta a}} \delta_a \tag{5.2}$$

$$0 = C_{N_\beta} \beta + C_{N_{\delta r}} \delta_r + C_{N_{\delta a}} \delta_a \tag{5.3}$$

$$0 = C_{l_\beta} \beta + C_{l_{\delta r}} \delta_r + C_{l_{\delta a}} \delta_a \tag{5.4}$$

From data supplied by the manufacturer of the full-scale Pioneer stability and control derivatives, values of β, δ_r, and δ_a were extracted from the above equations by varying ϕ [Ref. 10:p. 45]. These data were plotted in Figures 5.5 and 5.6 with slopes of 0.523 and -0.870, respectively. Likewise, stability and control derivatives from wind tunnel tests were substituted into Equations 5.2, 5.3, and 5.4, and the resulting lines were plotted having slopes of 1.154 for

rudder deflections and -0.1593 for aileron deflections [Ref. 8:p. 33]. Finally, data extracted from computational methods were plotted. The line in Figure 5.5 has a slope of 1.288 [Ref. 9:p. 39]. A panel analysis was not used to investigate aileron effects.

The flight test data correlated well with the wind tunnel data and the panel-code data; the manufacturer's data did not correspond well. The source of data collection used by the manufacturer was not known. Although the wind tunnel tests were performed on a 0.4-scale Pioneer at full-scale Reynolds numbers with a large tail, and the computational method was done for a full-scale, small tail Pioneer, the results should be directly comparable with the flight test data from the half-scale, small tail Pioneer. The rudders, in each case, were geometrically similar and should have had the same effects on flight characteristics, as discussed in Chapter II. Because the computational method did not include aileron effects, there was some question of whether these data would be valid for comparison. Equation 5.5 shows the relationship between yaw moment, side slip, and control deflections.

$$C_N = C_{N_\beta}\beta + C_{N_{\delta r}}\delta_r + C_{N_{\delta a}}\delta_a \qquad (5.5)$$

For steady flight, C_N is zero. When stability and control derivatives supplied by the manufacturer were substituted into Equation 5.5, the last term is at least an order of magnitude less than the other terms. The same results were achieved using the wind tunnel data from Reference 8. The last term in the equation was therefore neglected and the panel method data could also be used in the above comparisons. [Ref. 15:p. 75]

VI. CONCLUSIONS AND RECOMMENDATIONS

A. CONCLUSIONS

The hardware changes to the Pioneer seemed to be robust enough to withstand the vibration levels present in the Pioneer, and no material failures were experienced. The integration of the telemetry transmitter was successful, as well. The entire data collection system should be capable of expanding to include other types of data sensors, such as an altimeter or rate gyros. However, the telemetry system does need further tuning to expand its voltage input range, which will be addressed in the recommendation section of this chapter.

Even though the flight test data were scattered, in most cases, the telemetry system appeared to function properly. The side slip data, pertaining to rudder deflections, plotted linearly with a very low degree of scatter. The reason that the rudder deflection data plotted so well is most likely because the rudder experienced the greatest amounts of deflection. The rudders moved over 20° in each direction, while the ailerons moved less than 5° maximum for the data run that used full left rudder. Likewise, in the longitudinal tests, the elevator moved barely 4° at the slowest airspeed with the cg forward.

There also seems to be an inherent difficulty with performing RPV longitudinal flight tests. This type of test requires that the airspeed be very steady and that the aircraft be held in straight and level flight, with no perturbations of the flight controls. This degree of steadiness is extremely difficult to achieve, even for the most proficient pilot, when there are no instruments available to analyze flight conditions. Coupled with the low

resolution from the elevator output signal, the longitudinal flight test data were very difficult to accurately acquire.

B. RECOMMENDATIONS

To better characterize the static stability of the Pioneer, more flight testing needs to be conducted. There simply are not enough data available to characterize the stability, especially longitudinal stability.

Before further flight tests are conducted, the quality of the data can be enhanced through several changes in the data collection hardware. Since the deflections of the ailerons and rudder were relatively small, the gear sets should be reinstalled at those locations. With the magnitude of those control surface deflections being small, the voltage range of the telemetry transmitter will not be exceeded. Also, the telemetry transmitter encoder module should be modified to accept as close to a five-volt input range as practical. This modification would allow gear sets to be installed on all control surfaces and the airspeed indicator would be useable over its range.

Finally, the REDUCE program used for data reduction should be modified to be more generic. The program should allow for generic calibration files to be input rather than the specifically named files written into the code. The program should also be changed to allow more than three calibration points to be used for creating the calibration file. The airspeed indicator output follows a third degree polynomial that would require four calibration points for using the entire curve. For the linear portion of the curve used in this flight test, three calibration points were acceptable.

APPENDIX A: ELECTRICAL SCHEMATICS

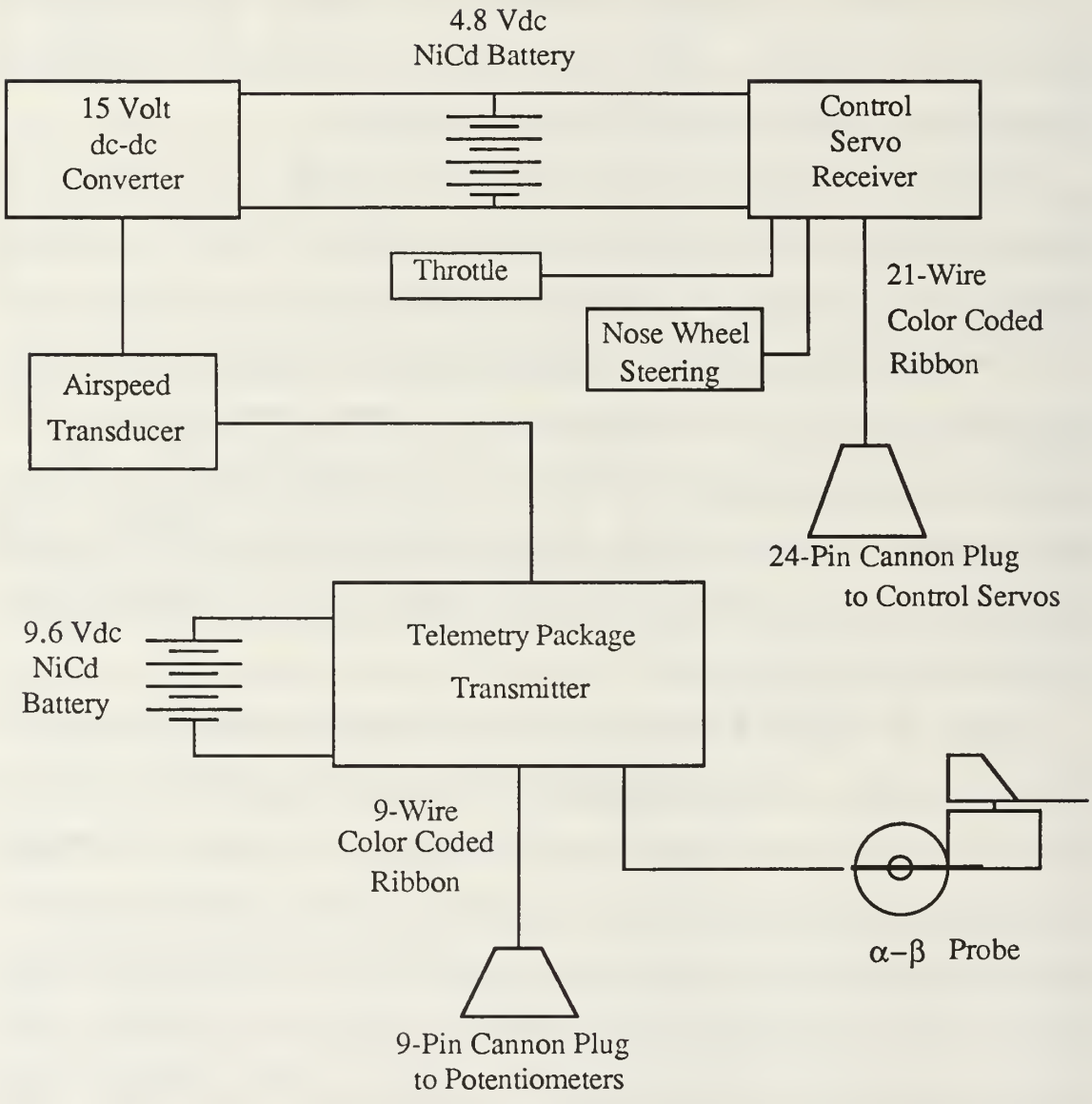

Figure A.1: Electrical System

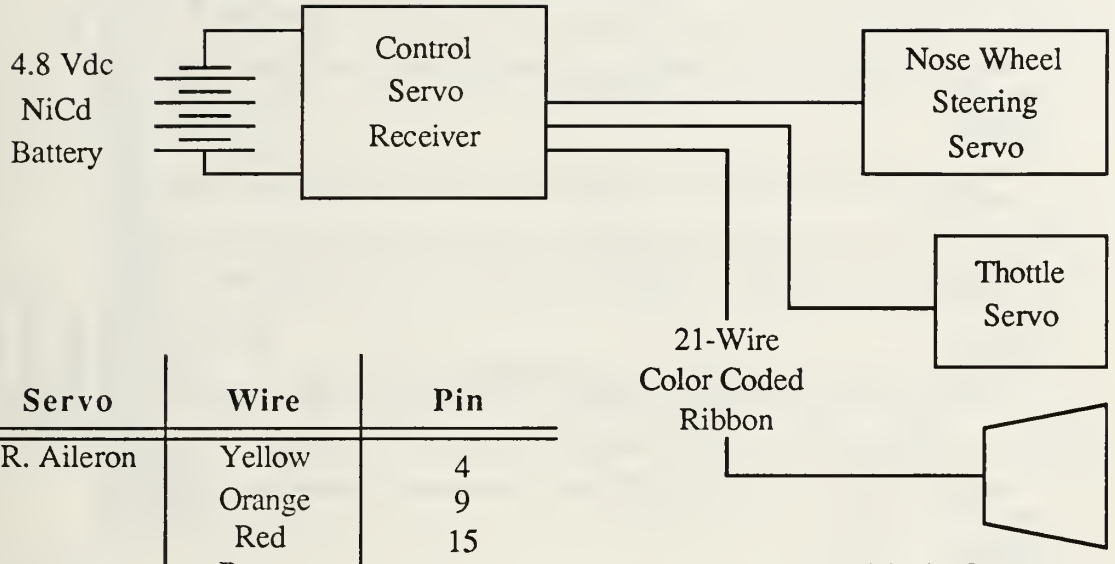

Servo	Wire	Pin
R. Aileron	Yellow	4
	Orange	9
	Red	15
L. Aileron	Brown	14
	Black	8
	White	3
R. Flap	Grey	2
	Purple	7
	Blue	13
L. Flap	Green	12
	Yellow	6
	Orange	1
R. Rudder	Red	5
	Brown	11
	Black	10
L. Rudder	White	16
	Grey	21
	Purple	17
Elevator	Blue	22
	Green	18
	Yellow	23
Blank	——	19, 20, 24

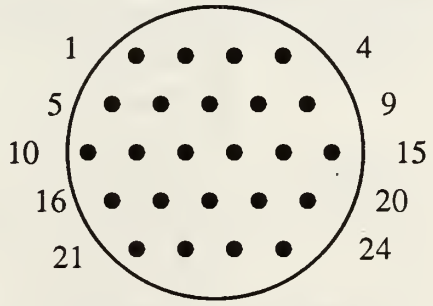

Cannon Plug Pin
Numbering Sequence

Figure A.2: Flight Control System

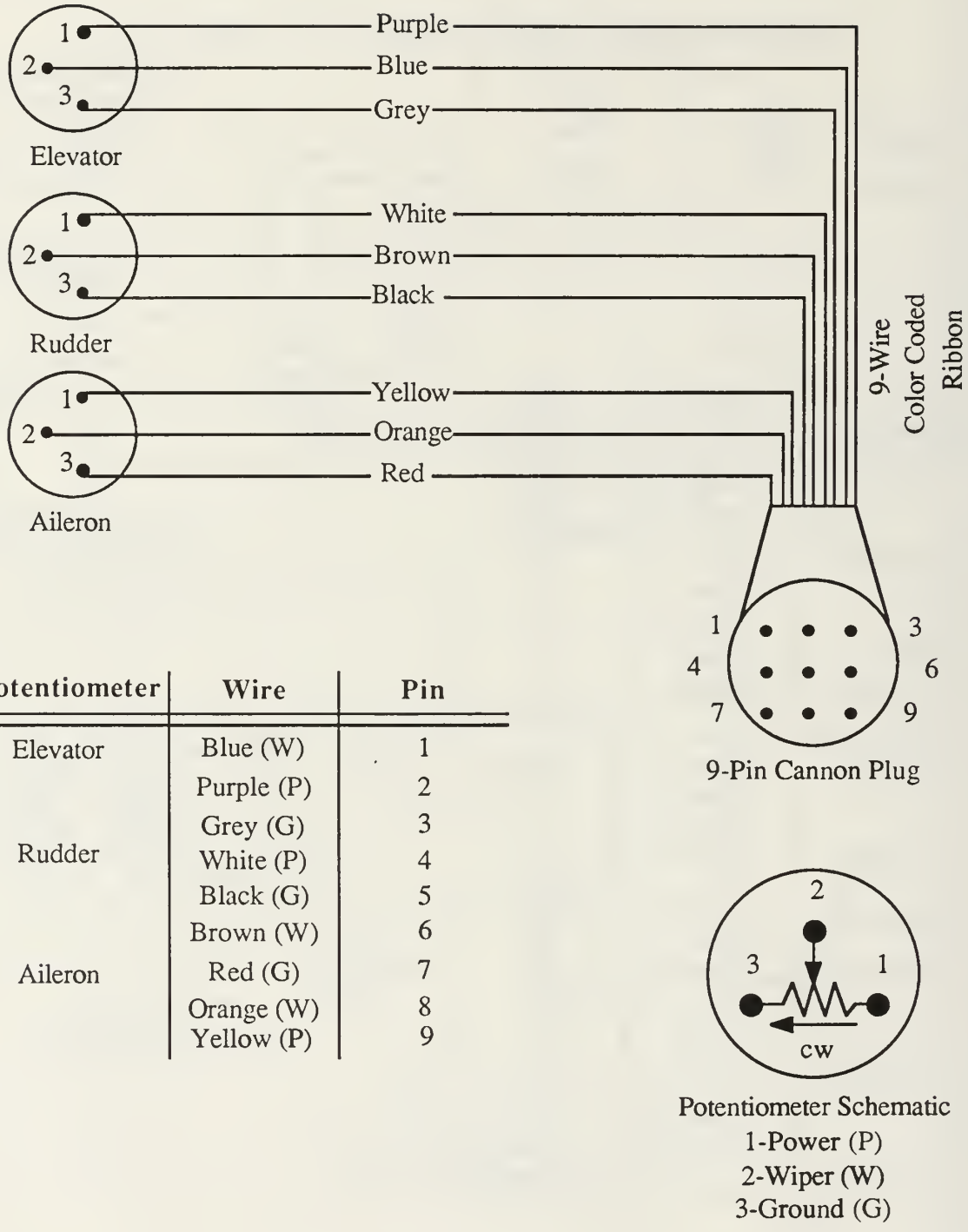

Potentiometer	Wire	Pin
Elevator	Blue (W)	1
	Purple (P)	2
	Grey (G)	3
Rudder	White (P)	4
	Black (G)	5
	Brown (W)	6
Aileron	Red (G)	7
	Orange (W)	8
	Yellow (P)	9

Figure A.3: Data Collection System

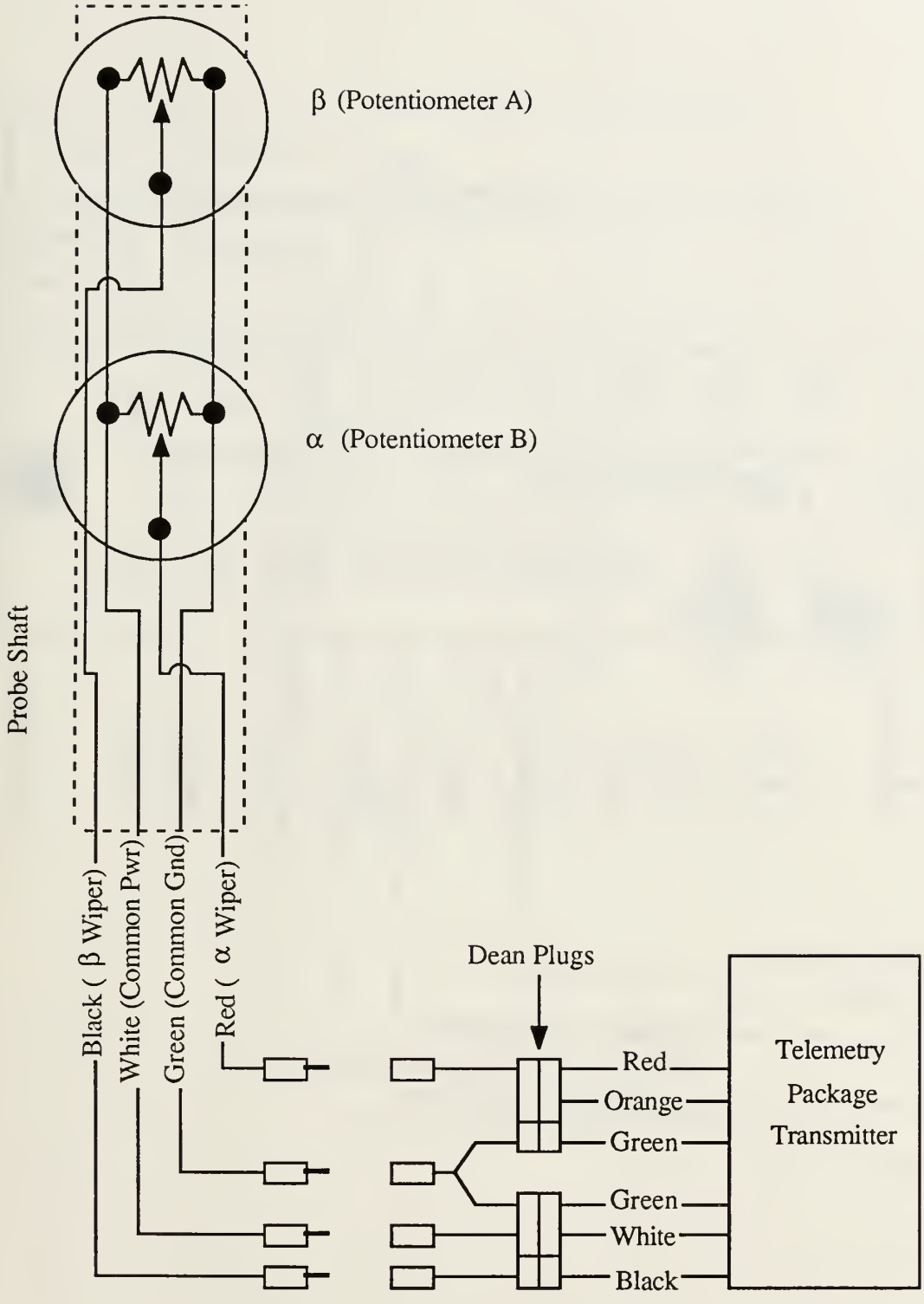

Figure A.4: α-β Probe

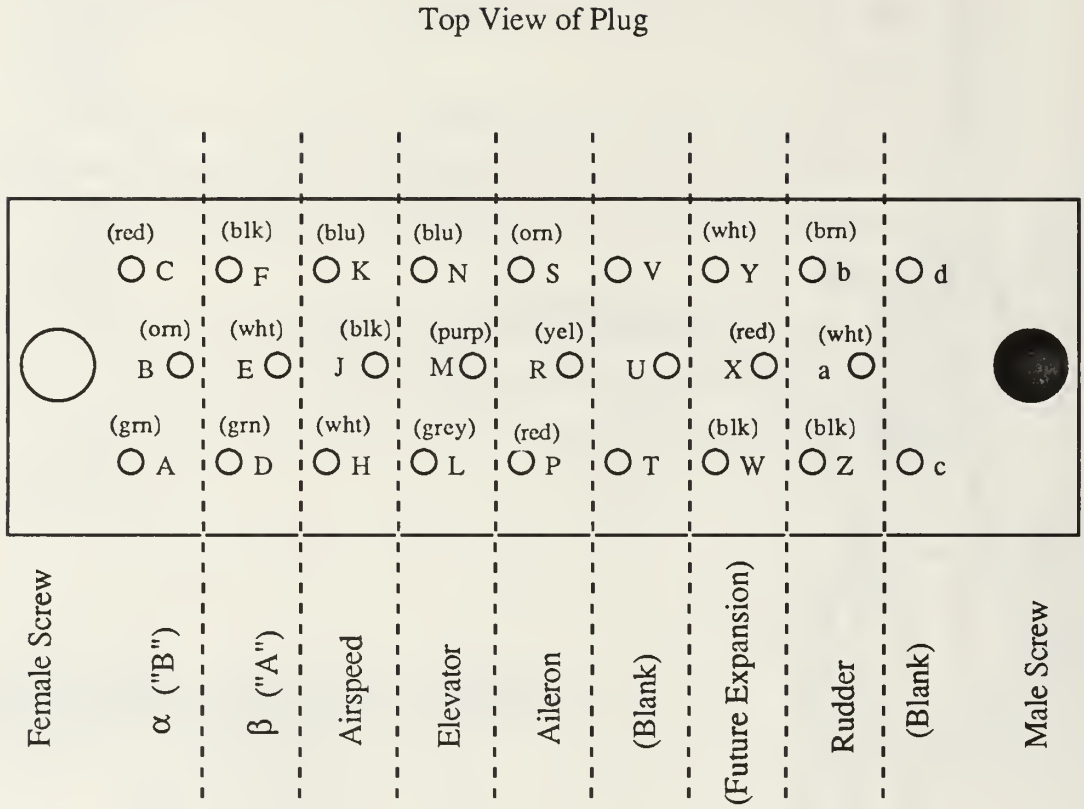

Top Row: Wiper Pins
Middle Row: +5Vdc Power Supply Pins
Bottom Row: Ground Pins

Figure A.5: Telemetry Transmitter Input Plug

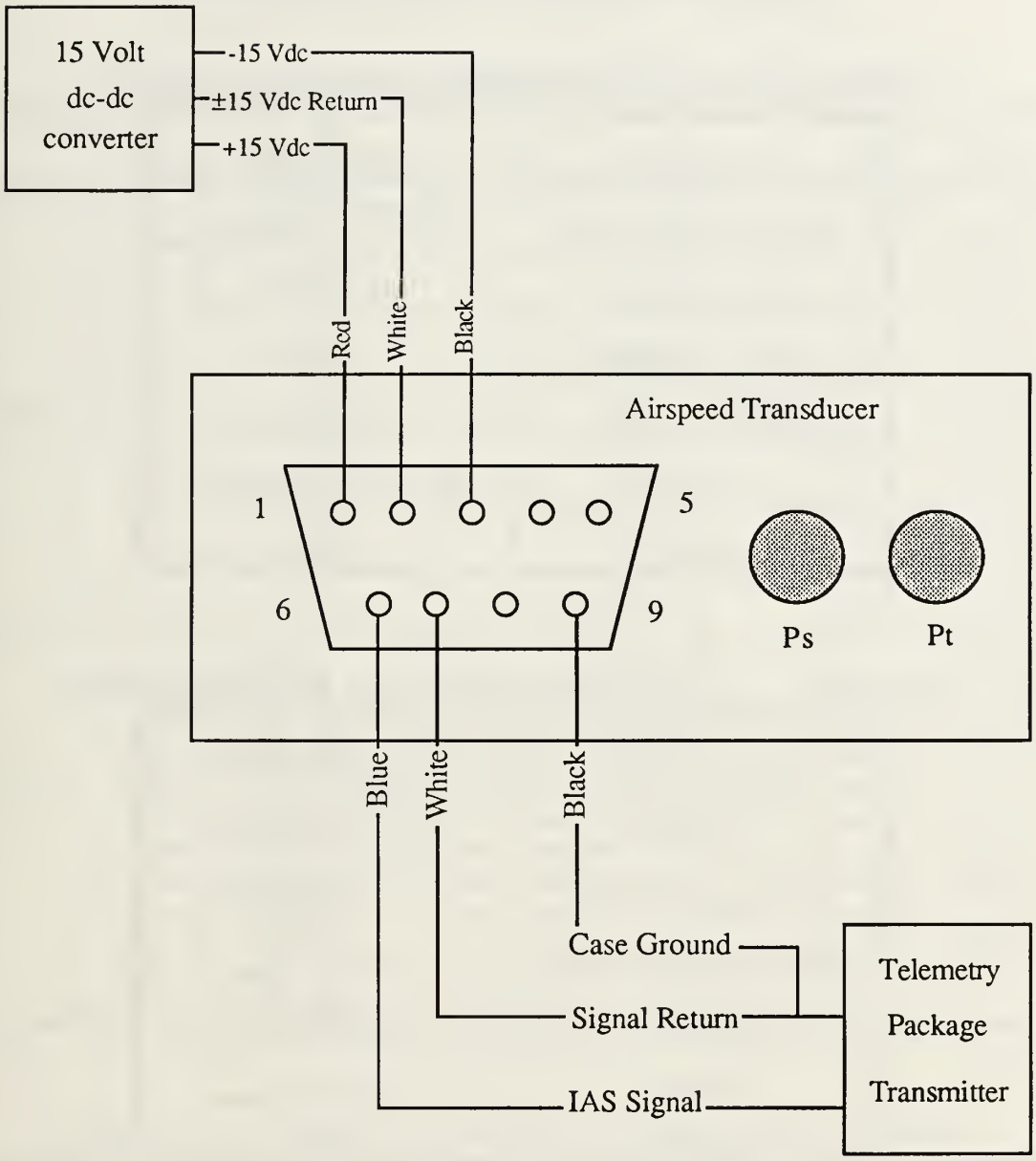

Figure A.6: Airspeed System

APPENDIX B: SPECIFICATIONS

TABLE B.1: POTENTIOMETER SPECIFICATIONS

Description	Specification
Temperature Range	-55°C to +125°C
Rotation Angle	330°±5°
Body Diameter	1/2 in
Shaft Diameter	1/8 in
Vibration	20 g, 10 to 2000 Hz
Shock	50 g

TABLE B.2: AIRSPEED TRANSDUCER SPECIFICATIONS

Description	**Specification**
IAS Range	30 to 130 Knots
Voltage Gradient	75 mVdc/Knot
Power Requirement	±15 Vdc
Length	3.188 in
Height	1.188 in
Depth	1.650 in
Weight	6.0 oz
Temperature Range	-55°C to +71°C
Vibration	10 g, 5 - 2000 Hz
Shock Resistance	15 g

APPENDIX C: CALIBRATION DATA

TABLE C.1: CONTROL SURFACE CALIBRATION DATA

	δ_r	Vdc		δ_e	Vdc		δ_a	Vdc
	30	4.92					27	4.70
	25	4.44					25	4.56
	20	4.04		20	3.87		20	4.08
TEL	15	3.69	TED	15	3.57	TED	15	3.63
	10	3.28		10	3.24		10	3.27
	5	2.92		5	2.96		5	2.89
	0°	2.61		0°	2.62		0°	2.49
	-5	2.26		-5	2.29		-5	2.13
	-10	1.88		-10	1.96		-10	1.62
TER	-15	1.53	TEU	-15	1.60	TEU	-15	1.33
	-20	1.21					-20	0.85
	-25	0.83					-22	0.70
	-30	0.48						

TABLE C.2: CALIBRATION DATA WITH CONTROL ARMS

δ_r	Vdc	ms	δ_e	Vdc	ms	δ_a	Vdc	ms
30° TEL	4.98	1.50	15°TED	4.43	1.25	18°TED	4.75	1.40
0°	3.90	1.00	0°	3.93	1.00	0°	3.96	1.00
25°TER	3.19	0.65	20°TEU	3.35	0.70	18°TEU	3.35	0.70

TABLE C.3: α-β PROBE CALIBRATION DATA

α	Vdc	β	Vdc
45	3.13	45	1.94
40	3.05	40	2.01
35	2.97	35	2.10
30	2.90	30	2.17
25	2.83	25	2.25
20	2.75	20	2.32
15	2.68	15	2.40
10	2.59	10	2.47
5	2.52	5	2.55
0°	2.45	0°	2.62
-5	2.35	-5	2.69
-10	2.30	-10	2.77
-15	2.23	-15	2.84
-20	2.15	-20	2.91
-25	2.09	-25	2.97
-30	2.01	-30	3.05
-35	1.94	-35	3.12
-40	1.86	-40	3.20
-45	1.79	-45	3.26

TABLE C.4: AIRSPEED TRANSDUCER CALIBRATION DATA

cm of H_2O	Vdc	KIAS	cm of H_2O	Vdc	KIAS
.0	1.78	.0	13.7	6.89	90.8
.7	2.21	20.5	14.7	7.16	94.0
1.7	2.71	32.0	15.7	7.39	97.2
2.7	3.20	40.3	16.7	7.64	100.2
3.7	3.60	47.2	17.7	7.86	103.2
4.7	4.02	53.2	18.7	8.08	106.1
5.7	4.39	58.6	19.7	8.30	108.9
6.7	4.74	63.5	20.7	8.47	111.6
7.7	5.08	68.1	21.7	8.67	114.3
8.7	5.43	72.4	22.7	8.85	116.9
9.7	5.74	76.4	23.7	9.02	119.4
10.7	6.05	80.2	24.7	9.15	121.9
11.7	6.35	83.9	25.7	9.25	124.4
12.7	6.63	87.4			

APPENDIX D: FLIGHT TEST DATA

TABLE D.1: FLIGHT TEST DATA FOR LONGITUDINAL STABILITY

cg	α	β	δ_e	δ_a	δ_r	KIAS
30.0%	-0.1875	-	-3.3924	-0.6412	0.8237	70.8614
	-1.2912	-	-3.1413	-0.7402	0.6515	58.9140
	-3.7287	-	-4.0555	-0.3522	1.2809	56.1485*
	-4.9335	-	-3.8706	-0.5590	0.9979	56.0590*
33.4%	-0.4808	-	-1.9296	0.0470	1.5477	65.6163
	-0.1427	-	-1.8318	-0.3546	0.9447	62.9867
	-3.4961	-	-2.6980	-0.3538	-2.7264	55.8244*
	-4.7805	-	-3.4993	-0.3153	0.9486	55.8791*
36.1%	0.7542	-	-1.4538	0.1447	0.7452	75.3488
	0.4964	-	-0.9700	-0.1009	0.1904	60.5804

TABLE D.2: FLIGHT TEST DATA FOR DIRECTIONAL STABILITY

cg	α	β	δ_e	δ_a	δ_r	KIAS
33.4%	-0.1707	8.3761	-3.0912	0.3085	7.5832	61.0421
	-0.9596	15.0080	-0.2424	-4.8227	23.3095	56.1896*
	1.0216	-0.6518	-3.1898	-0.8412	-1.1442	70.6261
	-0.2274	-7.9412	-1.6567	-1.4533	-15.3280	57.3504
	-0.7442	-13.7969	-2.0273	3.2201	-20.1898	55.3849*

APPENDIX E: CHECKLISTS

EQUIPMENT

Airplane

_____ Fuselage

_____ Wing and Screws

_____ Tail and screws

_____ Access Panel Covers and Screws

_____ α-β Probe, locking nut and pin

_____ Flight Control Receiver Battery

_____ Chocks

Telemetry

_____ Transmitter and Battery

_____ Receiver Case and Battery

_____ Recorder and Battery

_____ Tapes

Flight Box

_____ Flight Control Transmitter and Battery

_____ Extra Battery

_____ Fuel and Pump

_____ Starter and Battery

_____ Extra Glow Plugs

_____ Ignitors

Tools/Miscellaneous

_____ Shop Tool Kit

_____ Tire Pump

_____ Wiring Harness, All

_____ Calibration Tools

_____ Ballast (cg test)

_____ Extra Rubber Bands

_____ Manometer

_____ Cleaner

_____ Paper Towels

_____ Hearing Protectors

Paper Work

_____ Flight Profiles

_____ Data Sheets

_____ Pencils

_____ Schedule Field

Most Important Item

_____ Donuts

2nd Most Important Item

_____ Coffee

BATTERY CHARGING

_____ Flight Control Receiver - 4.8 Vdc, 4000 mAh

_____ Flight Control Transmitter - 9.6 Vdc, 500 mAh

_____ Extra Transmitter Battery - 9.6 Vdc, 500 mAh

_____ Telemetry Transmitter - 9.6 Vdc, 500 mAh

_____ Telemetry Receiver - 9.6 Vdc, 800 mAh

_____ Video Camera Battery

_____ Extra Data Tape Recorder Battery

PREFLIGHT CHECKS

1.) Connect Airspeed Pressure Lines

2.) Attach Wing, Tighten Bolts

3.) Connect Tail Servo/Pot Leads

4.) Attach Tail, Tighten Bolts

5.) Connect Servo/Pot Cannon Plugs

6.) Secure Wiring Harness

7.) Install Telemetry Transmitter, Route Antenna

8.) Connect Battery to Transmitter

9.) Check Flight Control Battery

10.) Install α-β Probe

11.) Install Probe Locking Pin

12.) Tighten Probe Nut

13.) Attach Probe Wiring Harness

14.) Check All Electrical Switches Off

15.) Check Security of All Equipment in Fuselage

CALIBRATION CHECKS

1.) Connect "Schmidter"
2.) Flight Control Receiver Power - On
3.) Airspeed Power - On
4.) T/M Transmitter Power - On
5.) Transmit Switch - On
6.) Telemetry Receiver - On
7.) Data Recorder - On/Record
8.) Calibration as per Table
9.) All Power Switches - Off
10.) Disconnect "Schmidter"

Calibration Table:

Parameter	1st Point	2nd Point	3rd Point
α	+30°	0	-30°
β	+30°	0	-30°
Elevator	(+) TED	0	TEU
Aileron	(+) TED	0	TEU
Rudder	(+)TEL	0	TER
Pressure	Low	Medium	High

TAKEOFF CHECKS

1.) Check Fuel Level
2.) Check Servo Integrity, Remove Flags
3.) T/M Transmitter Battery - On
4.) T/M Transmit Switch - On
5.) Flight Control Receiver Power - On
6.) Airspeed Power - On
7.) Check Cockpit Security
8.) Close Access Covers
9.) Start Aircraft
10.) Telemetry Receiver - On
11.) Cycle Controls
12.) Check Telemetry Reception
13.) Tape Recorder - On/Record
14.) Note Takeoff Time

FLIGHT TEST CARD

Date: _____

Flight Test: _____

T/O Time: _____ Land Time: _____

(***** 15 Minutes Maximum Flight Time *****)

Toggle Flight Recorder Marker Each Pass When On Parameters

Pass 1: _____

Pass 2: _____

Pass 3: _____

Pass 4: _____

Pass 5: _____

Remarks: _____

_____

_____

_____

_____

_____

_____

_____

Flight Conditions:

Press: _____ Temp: _____ Elev: _____ Wind: _____

LIST OF REFERENCES

1. Clausawitz,Karl von,"On War," Princeton University Press, 1976.

2. Karch, Lawrance G., "CAS, SEAD and UAV's," Marine Corps Gazette, February, 1990.

3. Philpot, Tom, "Unmanned 'Toy' Played Big Role in U.S. Targeting of Iraqi Forces," Navy Times, March 11, 1991.

4. Anonymous, "Gulf War Experience Sparks Review of RPV Priorities," Aviation Week and Space Technology, April 22, 1991.

5. Hall, Stan, "Dynamic Modeling," Sport Aviation, July, 1987.

6. Anderson, John D., "Fundamentals of Aerodynamics," McGraw Hill, Inc., 1984.

7. Tanner, James C., "Development of Flight Test Methodology for a U.S. Navy Half-Scale Unmanned Air Vehicle," Master's Thesis, Naval Postgraduate School, Monterey, California, March, 1989.

8. Bray, Robert M., "A Wind Tunnel Study of the Pioneer Remotely Piloted Vehicle," Master's Thesis, Naval Postgraduate School, Monterey, California, June, 1991.

9. Lyons, Daniel F., "Aerodynamic Analysis of a U.S. Navy and Marine Corps Unmanned Air Vehicle," Master's Thesis, Navy Postgraduate School, Monterey, California, June, 1989.

10. Salmons, James D., "Developmental Flight Testing of a Half-Scale Unmanned Air Vehicle," Master's Thesis, Navy Postgraduate School, Monterey, California, September, 1990.

11. Howard, Richard M, Lyons, Danial F., Tanner, James C., "Research Flight Test of a Scaled Unmanned Air Vehicle," Society of Flight Test Engineers 21st Annual Symposium Proceedings, 1990.

12. Wilhelm, Kevin T., "Development and Testing of an Unmanned Air Vehicle Telemetry System," Master's Thesis, Naval Postgraduate School, Monterey, California, September, 1991.

13. Roberts, Sean C., "Flying Qualities Flight Testing of Light Aircraft for Test Pilots and Engineers," Flight Research, Inc., 1982.

14. Anderson, John D., "Introduction to Flight," McGraw-Hill,Inc., 1989.

15. Etkin, Bernard, "Dynamics of Flight - Stability and Control," John Wiley & Sons, 1982.

INITIAL DISTRIBUTION LIST

		No. Copies
1.	Defense Technical Information Center Cameron Station Alexandria, Virginia 22314-6145	2
2.	Library, Code 52 Naval Postgraduate School Monterey, California 93943-5002	2
3.	Chairman, Code AA Department of Aeronautics and Astronautics Naval Postgraduate School Monterey, California 93943-5000	1
4.	Professor Richard M. Howard, Code AAHo Department of Aeronautics and Astronautics Naval Postgraduate School Monterey, California 93943-5100	3
5.	LT Kent R. Aitcheson 919 Longridge Road Oakland, California 94610	2
6.	Mr. Richard J. Foch Naval Research Laboratory Code 5712 4555 Overlook Avenue, S.W. Washington, D.C. 20374	1
7.	Mr. David Lewis Unmanned Aerial Vehicles Joint Project PEO (CU)-UD Washington, D.C. 20361-1014	1

8. Short-Range Program 1
Unmanned Aerial Vehicles Joint Project
PMA 263
Washington, D.C. 20361-1263

Thesis
A32 Aitcheson
c.1 Stability and control flight testing of a half-scale Pioneer remotely piloted vehicle.